A STUDY ON THE SOLUBILITY OF HEAVY HYDROCARBONS IN LIQUID METHANE AND METHANE CONTAINING MIXTURES

by

T.C.L. BREW

Thesis submitted to the School of Graduate Studies in partial fulfillment of the requirements for the degree of Master of Applied Science in the Department of Chemical Engineering.

UNIVERSITY OF OTTAWA

OTTAWA, CANADA, 1977

ABSTRACT

The solubilities of the hydrocarbons n-butane, n-pentane, n-hexane, n-octane, and n-nonane in liquid methane and of n-hexane in the mixed solvents of methane and ethane and of methane and propane were obtained using a forced vapour recirculation apparatus.

The liquid phase was sampled and analysed by gas chromatography.

Liquid concentration ranges from 28.30 mole percent at 113.3K to 81.15 mole percent at 129.K for n-butane; from 5.09 mole percent at 123.4K to 41.19 mole percent at 131.25K for n-pentane; from 1.20 mole percent at 149.K to 17.95 mole percent at 166.2K for n-hexane; from 0.04 mole percent at 156.3K to 0.64 mole percent at 179.7K for n-octane; and from 0.03 mole percent at 161.6K to 0.18 mole percent at 184.3K for n-nonane.

The solubility of n-hexane in the mixed solvents methane-ethane and methane-propane were also determined in order to assess the enhancement effect of the solvents ethane and propane.

The n-hexane concentration in the mixed solvents were from 0.18 mole percent at 114K to 20.39 mole percent at 154.8K in the mixed solvents of methane and ethane and from 0.65 mole percent at 120.4K to 15.78 mole percent at 153.K in the mixed solvents of methane and propane.

An attempt was made to correlate the experimental results through the liquid activity coefficient which was calculated by means of the Redlich-Kwong equation of state with a modified procedure.

ACKNOWLEDGEMENT

The author wishes to express his sincere thanks and gratitude to his supervisor Professor B.C.-Y. Lu, for his advice, guidance, encouragement and constructive criticism during the course of this investigation.

Special thanks are due to Dr. W.K. Chung for his extensive programming assistance, to Mr. F. Giacobbi for his administrative help and to Messrs G. Gasperetti, A. Bonaldo and Denis Roy for their technical assistance.

The financial support provided by the Canadian Commonwealth Scholarship and Fellowship Plan is also gratefully acknowledged.

Gratitude is also extended to Mrs. S. Roy for the skillful typing.

TABLE OF CONTENTS

LIST OF TABLES

LIST OF FIGURES

NOMENCLATURE

A^2,B	adjustable parameters as defined by Equations 4.8 and 4.9
a_{ij}	cross coefficient as defined by Equation (3.49)
f	fugacity
G	Gibb's Free Energy
H	enthalpy
k_{ij}	interaction parameter as defined by $T_{cij} = (T_{ci}\ T_{cj})^{0.5}\ (1-k_{ij})$
P	pressure
R	Universal Gas Constant
S	entropy
T	temperature
V	volume
X	liquid phase mole fraction
Z	compressibility factor

Greek Letters

γ	activity coefficient
Δ	deviation
ϕ	fugacity coefficient
ω	acentric factor
Ω_a, Ω_b	parameters of the Redlich-Kwong Equation of state

Superscripts

o	standard state
l	liquid
v	vapour

s	solid
sat	saturated
^	property in solution

Subscripts

c	critical property
i,j or 1,2	component identification
ij	i-j pair
m or f	melting point property
t	triple point property
trans	transition point property
sc	scaling volume

CHAPTER 1. INTRODUCTION

Natural gas is a hydrocarbon mixture. Its major constituent is methane and the minor constituents are ethane, propane, butane, pentane and other heavy homologues of the alkane hydrocarbons series.

In addition to the constituents mentioned above, non hydrocarbon components such as nitrogen (N_2), hydrogen (H_2), carbon dioxide (CO_2), hydrogen sulphide (H_2S), water (H_2O) and traces of rare gases especially helium (He) occur.

In the past, natural gas found in inaccessible regions of the world were regarded as being of scant economic value and the wells from which they had been produced were plugged or abandoned. In situations where the gas was associated with considerable quantities of oil, the associated gas was either reinjected into the oil producing wells or it was flared.

However, concern about atmospheric pollution and conservation of the environment, the economics of energy generation, the necessity for a fuller utilization of natural resources, the objections raised by the governments of oil-producing countries against the flaring of by-product gas from crude oil operations and the need to supply the ever growing demand for energy by both the developed and developing regions around the globe has resulted in a sudden spread of LNG production schemes and hence in a rapid increase in the demand for natural gas.

Annual world consumption exceeds 10^{12} m^3 [1]. It accounts for more than 18.5% of the worlds energy demand. World production increases at a rate of about 8% yearly.

North America produces and consumes about 68%[1], the U.S.S.R. and its allies about 22%[1], Western Europe about 4.5%, Middle and South America about 3.5%[1] and the Middle East, Africa, the Far East and Oceania about 2%[1] of the total world production.

The fact that natural gas is not as a rule produced in close proximity to regions of high gas demand has resulted in major movements of gas by pipeline from gas fields to the centres of consumption.

Pipelines and piped gas transport have a number of drawbacks

(i) Pipelines cannot be laid at depths more than 100m below sea level and in any case underwater pipelines are expensive and sometimes at risk.

(ii) Political conditions in the areas between producer country and centres of gas consumption may not be conducive to investment.

(iii) Pipelines are permanent fixtures leading from a given gas field to a particular consuming area, whereas both sources of gas and concentrations of gas consumption are subject to change.

(iv) Finally gas stored in a pipeline under pressure can be utilized to a limited extent to follow fluctuating gas demand by allowing pressure changes in the line.

Liquified natural gas on the other hand is

(i) Ideally transported across the sea, although road, rail and particularly barge movements are operational in various parts of the world.

(ii) Transport from field to consumer is therefore largely across the open sea and is unhampered by political instability en route.

(iii) And while liquefaction plants and loading facilities are permanently tied to a particular gas field, the LNG ships which represent the largest investment in an LNG scheme can be moved from one supply system to another.

(iv) Similarly, the destination of the LNG once it is loaded can be changed in accordance with demand. A particular instance is seasonal gas demand in the Northern and Southern hemispheres.

Finally liquified natural gas (LNG), once produced and refrigerated can be stored at atmospheric pressure and therefore constitutes a useful gas reserve to be drawn upon when the demand temporarily rises above average.

One of the processing difficulties that is encountered at natural gas liquefaction plants is the formation and precipitation of solid hydrocarbons in the liquefaction units for Liquified Natural Gas. These solids can coat the surfaces of heat exchangers and foul turbo-expansion devices thus requiring the unit to be shut down for cleaning and/or repair. Reliable phase equilibrium data are essential for

the design of efficient and economical liquefaction units and it is the goal of this project to study the solubility of heavy hydrocarbons in Liquefied Natural Gas with the view to

(i) Enlarging the body of hydrocarbon solubility data in liquefied natural gas or in liquid methane.

(ii) Attempting to develop a method for correlating the experimental results and thereby reducing the number of experimental determinations in the future.

The solubility limits of the hydrocarbons studied are generally quite low at the temperatures of interest. Consequently, the focus of the data taking has been on the low concentration range of solubility behaviour.

In addition a limited amount of ternary data for the systems methane-ethane-n-hexane and methane-propane-n-hexane will be taken in order to assess the enhancement effect of the two hydrocarbons, ethane and propane on the solubility of n-hexane.

The solubility of n-hexane in the mixed solvents methane-ethane and methane-propane were determined because no data on these systems existed in the literature and also the systems, methane-ethane-n-hexane and methane-propane-n-hexane were not included in the solubility data on single solutes in mixed solvents [4] and two solutes in a single solvent [4] which became available while this investigation was in progress.

CHAPTER 2. LITERATURE SURVEY

A review of solubility data for solids in cryogenic solvents [2] by Prausnitz showed that while solubility data in liquid methane are somewhat plentiful, few measurements have however, been made at low temperatures for hydrocarbons larger than propane.

The paucity of solubility data of heavy hydrocarbons in liquid methane could probably be attributed to the fact that even though natural gas has been known to exist for a long time and has enjoyed limited utility, its utilization on a large scale both in its original and new form LNG dates back to the last two decades or so. As such the need for data relevant to the design of LNG production units arose at about the same time.

The available data in the literature for the period 1954 to 1973 have been collected together and published [3] by Kurata for easy reference.

A summary of the literature data reviewed is presented in Table 2.1.

TABLE 2.1

SUMMARY OF LITERATURE DATA

System	T K	P,Psia	Reference
Methane-n-Butane	117.4-134.8	-	Kurata (1954-56) [3]
	106.3-127.6	17.1-19.7	Kuebler & McKinley (1975)
Methane-n-Pentane	100.4-124.5	-	Preston, Funk and Prausnitz (1971) [2]
	119.3-138.5	-	Kurata (1954-56) [3]
	116.5-139.8	21.1-49.6	Kuebler & McKinley (1975)
Methane-n-Hexane	124.3-176.8	-	Beck (1956) [3]
	162.9-176.6	-	Shim and Kohn (1962) [3]
	127.4-163.7	1024-1524	Kuebler and McKinley (1973) [3]
Methane-n-Octane	208.8-215.5	-	Papahronis (1954) [3]
	205.6-216.5	-	Kohn and Bradish (1964) [3]
	155.0-191.0	202.2-692.	Kohn and Luks (1976) [4]
Methane-n-Nonane	208.36-219.36	-	Shipman and Kohn (1966) [3]
Methane-Ethane-n-Heptane	150.83-179.17	244.4-379.2	Kohn and Luks (1976) [4]
Methane-Ethane-n-Octane	159.28-192.79	200.2-580.5	" " "
Ethane-n-Hexane-n-Dodecane	218.72-233.78	80.4-88.3	" " "
Methane-Ethane-n-Hexane-n-Octane	178.29-185.73	407.4-461.3	" " "
Methane-Ethane-n-Hexane-n-Heptane-n-Octane	166.47-180.28	378.6-442.5	" " "

An examination of the solubility data compiled and the solubility curves drawn by Kurata [3] showed that the available solubility data were inadequate since portions of the solubility curves were devoid of data points. To remedy this inadequacy or insufficiency of solubility data was one of the objectives of this undertaking.

The second objective was, it was hoped, to resolve the discrepancy (see Figures 4.3 to 4.5) in the literature data.

Thirdly, prior to the commencement of this investigation no generalized correlation or a thermodynamic model capable of predicting solid formation conditions during the low temperature processing of natural gas has been reported.

However, an attempt [13] at correlating experimental solubility data through the liquid activity coefficient has been made.

The absence of a generalized correlation or predictive model does not imply that work at realizing such objectives were not in progress for in 1976, Kohn and Luks [4] reported that they have succeeded in developing a computer package or model capable of predicting solid formation conditions during the low temperature processing of natural gas.

The third objective of this investigation will therefore be to attempt to correlate our experimental data and if possible some of the literature data.

2.2 Experimental Techniques

From the literature survey it was found that either one or the other of two methods have been used in obtaining solubility data. The methods are namely,

(i) The isoplethal [5] or cryoscopic [4] method

(ii) The isothermal [5], analytical or sampling [4] method.

A description of the methods is given below:

2.2.1 The Isoplethal [5] or Cryoscopic [4] Method

In this method, mixtures of known composition are subjected to temperature changes. It is not widely used when the solubility is very low. The steps involved in this method are as follows:

(i) A graduated and transparent cell is charged with a known amount of the solute. The amount charged is established by accurate weighing techniques. After charging, air is flushed out of the cell by use of the solvent gas at 0°C. A few atmospheres of solvent gas pressure is left in the cell prior to inserting the cell in the pre-cooled dewar bath.

(ii) After mounting the cell in the bath, the solvent gas is added to the cell through a stainless-steel capillary tubing connected to the cell by an adaptor. The incremental amount and the cumulative amount of the solvent gas added to the cell is determined by means of a variable level mercury bomb. This bomb is maintained at constant

temperature and pressure so the volume of gas displaced could be translated into mass units.

(iii) The temperature of the cell is lowered until crystals of the solute appear in the liquid phase. During cooling agitation of the cell contents is achieved mechanically by raising and lowering a steel ball inside the cell by means of an external magnet.

(iv) At each crystal or equilibrium point, the temperature, pressure, liquid level and mass of solvent gas added to the cell are taken. These data permit a direct stoichiometric computation of the amount of the solvent gas dissolved in the liquid phase. Each addition of solvent gas to the equilibrium cell results in an additional crystal point at a lower temperature.

In general the cryoscopic method necessitates that the visibility through the equilibrium cell and the cryostat be good. Condensation of water on the dewar flask from the air in the laboratory sometimes reduces visibility. The cryoscopic method is not restricted to binary systems only. It has been applied [4] to mixed solvent gases and even mixed solute liquids as long as only one of the solute liquids crystallizes out at the temperature of interest.

2.2.2 Isothermal, Analytical or Sampling Method [5]

The use of gas chromatography, which allows accurate and convenient analysis of vaporized fluid mixtures, has

favoured the increased application of this method. Two steps are important in this method:

(i) Making the saturated solution.

(ii) Sampling of this solution for analysis.

A usual technique of preparing the solution is to agitate the mixture in the presence of excess solute by mechanical stirring or recirculation of the vapour phase. Failure to promote equilibration can result in systematic errors.

Solutions can also be formed using a single pass mode either with solute precipitating from a feed mixture or a previously deposited solute dissolved into a pure solvent feed stream. The resultant solution can be flash evaporated directly to ambient temperature or the solution can be transferred to a separate chamber and the entire apparatus warmed to ambient temperature.

Discrete samples taken from a bulk solution tend to be poorly reproducible especially in the parts per million range. Also the presence of minute quantities of highly soluble contaminants in the solute material can interfere with analysis by gas chromatograph.

An advantage of the continuously flowing sample stream is that the stream tends to leach out the highly soluble contaminants in the solute bed thus resulting in an uncluttered chromatogram.

Initial attempts [5], however, to use the single-pass continuous flow technique at pressures sufficient to

ensure liquefaction of the solvent stream yielded poor reproducibility and ultimate plugging of the sample line. These problems were eliminated by flowing the solvent above its critical pressure, thus avoiding the liquid to vapour transition in the sampling line.

The technique is also inherently suited to the investigation of the effect of pressure on solubility.

For this investigation a forced vapour recirculation apparatus generally used for vapour-liquid equilibrium (VLE) studies in this laboratory was used. Reasons for using this apparatus are:

(i) It was readily available and in working order.

(ii) It has been used to study the solubility of hydrocarbons in liquid methane in a preliminary investigation.

A description of the apparatus is given in chapter four.

CHAPTER 3. THEORETICAL CONSIDERATIONS

3.1 Thermodynamic Considerations

The criterion of equilibrium for a binary solid-liquid-vapour system is that for each component i, present, the equality as expressed by Equation (3.1) [7] holds,

$$\mu_{is} = \mu_{il} = \mu_{iv} \qquad 3.1$$

where μ_i is the chemical potential of component i.

Thus for a binary system 1, 2, where "1" denotes the solvent and "2" the solute application of Equation (3.1)[7] yields the following set of equations [4].

$$\mu_{1\ell}\ (T,P,x_1) = \mu_{1v}\ (T,P,y_1) \qquad 3.2$$

$$\mu_{2s}\ (T,P) = \mu_{2\ell}\ (T,P,x_2) \qquad 3.3$$

$$\mu_{2\ell}\ (T,P,x_2) = \mu_{2v}\ (T,P,y_2) \qquad 3.4$$

However, for practical purposes it is necessary to relate the chemical potential of the equilibrated phases to a certain auxilliary function known as the fugacity [6,7].

The fugacity of any component i of a solution $\hat{f}_i$ is defined by the equation (3.5) [6,7].

$$\mu_i = \mu_i^{\circ} + RT\ln\hat{f}_i$$

$$\frac{\hat{f}_i}{y_{iP}} \to 1 \text{ as } P \to o \qquad 3.5$$

where μ_i is a function of temperature only and has precisely the same value as for the pure component i at the same temperature and unit fugacity.

For solid-liquid-vapour equilibrium substitution of Equation (3.5) into Equations (3.2), (3.3) and (3.4) gives

$$\hat{f}_{1\ell} = \hat{f}_{1v} \qquad 3.6$$

$$\hat{f}_{2s} = \hat{f}_{2\ell} = \hat{f}_{2v} \qquad 3.7$$

Assuming that no solid solutions are formed and that the solid phase is the pure solid solute,

$$\hat{f}_{2s} = f_{2s} \qquad 3.8$$

therefore

$$f_{2s} = \hat{f}_{2\ell} \qquad 3.9$$

For an ideal solution

$$\hat{f}_{2\ell} = x_2 f_{2\ell} \qquad 3.10$$

substituting for $\hat{f}_{2\ell}$ in equation 3.9 gives

$$f_{2s} = x_2 f_{2\ell} \qquad 3.11$$

or

$$x_{2\,(IDEAL)} = \frac{f_{2s}}{\hat{f}_{2\ell}} \qquad 3.12$$

where $\hat{f}_{2\ell}$ is the fugacity of component 2 in solution, $f_{2\ell}$ is the fugacity of the pure subcooled liquid, x_2 is the mole fraction of solute in the saturated solution and f_{2s} is the fugacity of the pure solid solute. All of these terms are evaluated at the pressure P and temperature T of the system.

Assuming that the vapour pressure of the pure solid and of the subcooled liquid are not large, and since at low pressure f is equal to P; we can write[7]

$$x_{2(IDEAL)} = \frac{P^{\circ}_{2s\ (pure\ solid)}}{P^{\circ}_{2\ell\ (pure\ subcooled\ liquid)}} \qquad 3.13$$

Thus the ideal solubility of a solute "2", in a solvent at a given temperature can be evaluated if the vapour pressure of the pure solid and of the pure subcooled liquid solute are known.

The ideal solubility can also be evaluated using the Equation [8]

$$\ell n\ x_{2(IDEAL)} = \frac{\Delta S_f}{R}\ (1 - \frac{T_f}{T}) \qquad 3.14$$

where ΔS_f is the entropy of fusion

T_f is the fusion temperature

R is the gas constant

Equation 3.14 may be derived as follows:

The fugacity in two states A and B is related to the molar free energy G_A and G_B in these states by the equation [9]

$$G_B - G_A = \Delta G_{A\rightarrow B} = RT\ ln\ {}^{f_B}/_{f_A} \qquad 3.15$$

Since the solute in solution is a subcooled liquid we can write

$$\Delta G_{A\rightarrow D} = RT\ ln\ \frac{f_{2\ell}}{f_{2s}} \qquad 3.16$$

where A denotes the pure solid solute and D the pure subcooled liquid solute.

The molar free energy change $\Delta G_{A\rightarrow D}$ can be evaluated with the help of the following thermodyanmic path [7].

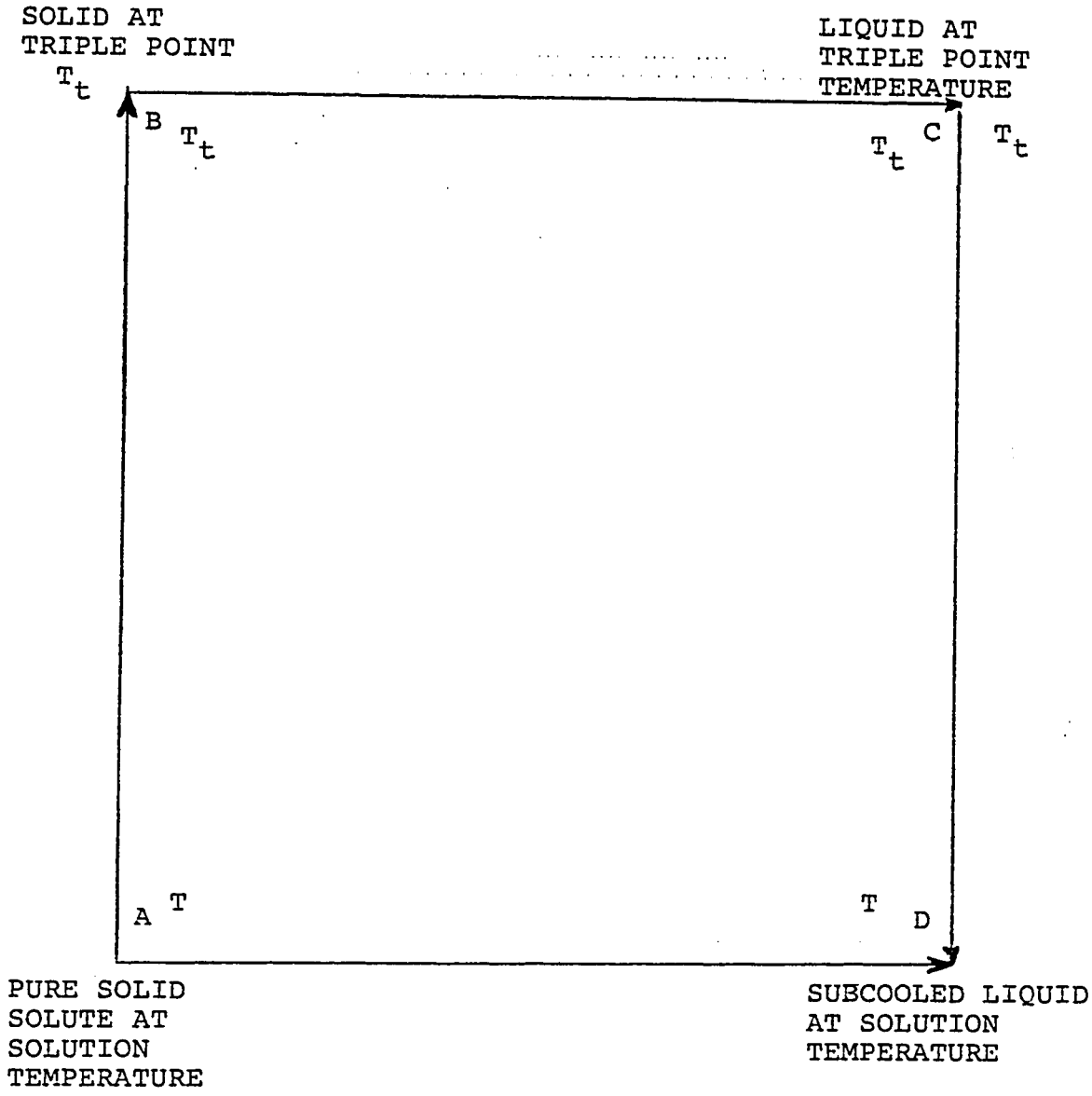

Figure 3.1 Thermodynamic Path[7] for Calculating the Fugacity of a Pure Subcooled Liquid.

The free energy change from state A to state D is given by

$$\Delta G_{A\to D} = \Delta H_{A\to D} - T\,\Delta S_{A\to D} \qquad 3.17$$

The enthalpy change from state A to D may be represented as

$$\Delta H_{A\to D} = \Delta H_{A\to B} + \Delta H_{B\to C} + \Delta H_{C\to D}$$

$$= \int_{T}^{T_t} C_{p(SOLID)}\, dT + \Delta H^{f}_{T_t} + \int_{T_t}^{T} C_{p(LIQUID)}\, dT$$

$$= \Delta H^{f}_{T_t} + \int_{T_t}^{T} \Delta C_p\, dT$$

which becomes after integration under the assumption that ΔC_p is constant

$$\Delta H_{A\to D} = \Delta H^{f}_{T_t} + \Delta C_p\,(T - T_t) \qquad 3.18$$

where $\Delta C_p = C_{pLIQUID} - C_{pSOLID}$

For the molar entropy change we may write

$$\Delta s_{A\to D} = \Delta s_{A\to B} + \Delta s_{B\to C} + \Delta s_{C\to D}$$

$$= \int_{T}^{T_t} \frac{C_{p(SOLID)}}{T}\, dT + \frac{\Delta H^{f}_{T_t}}{T_t} + \int_{T_t}^{T} \frac{C_{p(LIQUID)}}{T}\, dT$$

$$= \frac{\Delta H^{f}_{T_t}}{T_t} + \int_{T_t}^{T} \frac{\Delta C_p}{T}\, dT$$

which after integration under the assumption that ΔC_p is constant yields

$$\Delta S_{A\to D} = \frac{\Delta H^f_{T_t}}{T} + \Delta C_p \ln {}^{T}/_{T_t} \qquad 3.19$$

Substituting for $\Delta H_{A\to D}$ and $\Delta S_{A\to D}$ in the Equation 3.17 we get

$$\Delta G_{A\to D} = RT \ln \frac{f_{2\ell}}{f_{2s}} = \Delta H^f_{T_t} + \Delta C_p (T-T_t) - \Delta H^f_{T_t} ({}^{T}/_{T_t}) - T \cdot C_p \cdot \ln {}^{T}/_{T_t} \qquad 3.20$$

$$\therefore \ln {f_{2\ell}}/{f_{2s}} = \frac{\Delta H^f_{T_t}}{RT} \left(\frac{T_t}{T} - 1\right) - \Delta C_p \left(\frac{T_t}{T} - 1\right) + \Delta C_p \ln ({}^{T_t}/_{T}) \qquad 3.21$$

Now $$\frac{\Delta H^f_{T_t}}{RT_t} = \frac{\Delta S^f_{T_t}}{R} \qquad 3.22$$

substituting $\frac{\Delta S^f_{T_t}}{R}$ for $\frac{\Delta H^f_{T_t}}{RT_t}$ in Equation 3.21

We get

$$\ln \frac{f_{2s}}{f_{2\ell}} = \frac{\Delta S^f_{T_t}}{R} \left(1 - \frac{T_t}{T}\right) - \frac{\Delta C_p}{R} \left(1 - {T_t}/{T}\right) + \frac{\Delta C_p}{R} \ln {}^{T}/_{T_t} \qquad 3.23$$

Equation 3.23 can be simplified with the following assumptions. First, at saturated system pressure, T_t is nearly equal to the normal melting temperature T_f; secondly the molar entropy of fusion at T_f, ΔS_f is negligibly different from that at T_t; and since the two terms containing ΔC_p are opposite in sign, they tend to cancel each other out for temperatures not too far removed from the triple point. With these assumptions Equation 3.23 becomes

$$\ln \frac{f_{2s}}{f_{2\ell}} = \frac{\Delta S_f}{R} (1 - \frac{T_f}{T}) \qquad 3.24$$

For an ideal solution the ratio

$$\frac{f_{2s}}{f_{2\ell}} = x_{2(IDEAL)} \qquad 3.25$$

substitution of $x_{2(IDEAL)}$ for the ratio $\frac{f_{2s}}{f_{2\ell}}$ in Equation 3.24 gives

$$\ln x_{2(IDEAL)} = \frac{\Delta S_f}{R} (1 - \frac{T_f}{T}) \qquad 3.26$$

which is the same as Equation 3.14.

A very satisfactory representation of ideal solubility is to plot $\ln x_2$ against $1/T$ This gives nearly a straight line whose slope is $\frac{\Delta S_f}{R}$ and whose upper limit is $\ln x_2 = 0$, at the melting point of the solute. If the melting point of the solute is known together with a single point on the solubility curve, a straight line drawn through these two points will give very closely the solubility at other temperatures. If the heat of fusion of the solute is known it may be used to give the slope of the line and hence the ideal solubility curve.

When the solution is non-ideal Equation 3.25 is no longer valid. To restore validity, the mole fraction must be multiplied by the quantity γ, which is the activity coefficient.

3.2 Definition of the Liquid Phase Activity Coefficient

Deviations from ideal behaviour in the liquid phase can be described in terms of the activity coefficient. The fugacity of a component i in a liquid solution is related to the mole fraction x_i by an equation of the form.[7]

$$\hat{f}_{i\ell} = \gamma_i \, x_i \, f^{\circ}_{i\ell} \qquad 3.27$$

Where $f^{\circ}_{i\ell}$ is the fugacity of component i at an arbitrary condition known as the standard state. At any composition, the activity coefficient γ_i depends on the choice of the standard state and the numerical value of γ_i has no significance unless the numerical value of $f^{\circ}_{i\ell}$ is also specified.

Since the choice of the standard state is arbitrary, it is convenient to choose $f^{\circ}_{i\ell}$ such that γ_i assumes values close to unity and when γ_i is exactly equal to unity the solution is said to be ideal [7]. However, owing to the intimate relation between the activity coefficient and the standard state fugacity, the definition of solution ideality ($\gamma_i = 1$) is not complete unless the choice of standard state is clearly specified.

In the liquid phase the usual practice is to have the temperature of the system, a fixed composition and specified pressure as the independent variables which determine the standard state of a component. A convenient choice of the standard state is the pure liquid at the system temperature and a reference pressure, p°.

For a non-ideal solution the equality of the fugacity ratio $f_{2s}/f_{2\ell}$ and the mole fraction x_2, ceases to be valid. The new equality is given by Equation (3.29):

$$\frac{f_{2s}}{f_{2\ell}} = \gamma_2 x_2 \qquad 3.29$$

Where γ_2 is the liquid phase activity coefficient of the solute referred to the pure subcooled liquid solute at the system pressure, P.

Substitution of $\gamma_2 x_2$ for the ratio $f_{2s}/f_{2\ell}$ in Equation 3.24 gives

$$\ln \gamma_2 x_2 = \frac{\Delta S_f}{R} \left(1 - \frac{T_f}{T}\right) \qquad 3.30$$

Certain substances undergo solid phase transitions from one crystal structure to another; n-butane being a good example. If the system temperature T, is less than the transition temperature T_{trans}, another term must be added to Equation 3.30. The modified equation is

$$\ln \gamma_2 x_2 = \frac{\Delta S_f}{R} \left(1 - \frac{T_f}{T}\right) + \frac{\Delta S_{trans}}{R} \left(1 - \frac{T_{trans}}{T}\right) \qquad 3.31$$

At the system temperature, the terms on the right hand side of Equation 3.31 can be evaluated from pure component properties.

The activity coefficient γ_2 can therefore be evaluated since values of x_2 have been obtained from experimental measurements. Having evaluated the activity coefficient γ_2, of the solute from pure component properties and the

experimentally determined solubilities by means of Equation (3.31), it will, since we intend correlating our experimental results through the liquid activity coefficient, be evaluated again by means of the Redlich-Kwong equation of state with a modified procedure [11] via the defining equation [7],

$$\gamma_{i\ell} = \frac{f_{i\ell}\ (T,P,x_i)}{x_i\ f^{\circ}_{i\ell}\ (T,P)} \qquad 3.32$$

by rearrangement. In Equation 3.32

$$\gamma_i \to 1 \text{ as } x_i \to 1$$

$\hat{f}_{i\ell}\ (T,P,x)$ is the fugacity of component i in the liquid mixture at the solution temperature T and pressure P, and $f^{\circ}_{i\ell}\ (T,P)$ represents the fugacity of the pure liquid i at the system temperature T, and pressure P. To evaluate these two quantities an equation of state must be used and the equation of state chosen was that proposed by Redlich and Kwong [10], but with a modified set of mixing rules or procedures [11].

The Redlich-Kwong equation of state was selected as the working equation of state for the following reasons:

1. It is commonly considered the best of two-parameter equations proposed until now [12].
2. It can be used to calculate, with a good degree of accuracy, volumetric and thermal properties of pure compounds and mixtures.

3. Its parameters Ω_a and Ω_b are readily evaluated from vapour pressures and saturated liquid volumes.
4. The binary interaction constant is easily introduced.
5. It saves computing time.
6. It is the working equation of our research group.
7. Other workers have used it to correlate and predict the solubilities of solid hydrocarbons in liquid methane [13].

3.3 Redlich-Kwong Equation of State

The original Redlich-Kwong equation of state is as follows [10]:

$$P = \frac{RT}{(V-b)} - \frac{a}{T^{0.5}\,(V+b)\,V} \qquad 3.33$$

Where the constants a and b can be related to the critical temperature T_c and critical pressure P_c by

$$a = \Omega^{\circ}_a \frac{R^2 T_c^{2.5}}{P_c} \qquad 3.34$$

$$b = \Omega^{\circ}_b \frac{RT_c}{P_c} \qquad 3.35$$

where $\Omega^{\circ}_a = 0.4278$ 3.36

$\Omega^{\circ}_b = 0.0867$ 3.37

The Redlich-Kwong equation is a third degree equation and purely empirical in nature. It has no thermodynamic or kinetic basis, nor any phase rule incorporated in the expression [10].

It can also be written in the form

$$Z = \frac{1}{1-h} - \frac{A^2}{B}\left(\frac{h}{1+h}\right) \qquad 3.38$$

where $$h = \frac{b}{V} = \frac{BP}{Z} \qquad 3.39$$

$$A^2 = a/R^2T^{2.5} = \Omega_a T_c^{2.5}/P_c T^{2.5} \qquad 3.40$$

$$B = b/RT = \frac{\Omega_b T_c}{P_c T} \qquad 3.41$$

The original mixing rules of the Redlich-Kwong equation are

$$a_{mixture} = \sum_i \sum_j x_i x_j a_{ij} \qquad 3.42$$

$$b_{mixture} = \sum_i x_i b_i \qquad 3.43$$

and $$a_{ij} = (a_i a_j)^{1/2} \qquad 3.44$$

For this work Equation 3.44 will be modified slightly by the introduction of the binary interaction constant k_{ij}.

The modified set of mixing rules or procedures[11] are as follows:

$$a_{mix} = \sum_i \sum_j x_i x_j a_{ij} \qquad 3.45$$

$$b_{mix} = \sum_i x_i b_i \qquad 3.46$$

$$b_i = \Omega_{bi} RT_{ci}/P_{ci} \qquad 3.47$$

$$a_{ij} = \Omega_{aij} R^2 T_{cij}^{2.5}/P_{cij} \qquad 3.48$$

In these equations,

$$T_{cij} = (T_{ci}\ T_{cj})^{0.5}\ (1 - k_{ij}) \qquad 3.49$$

$$\Omega_{aij} = (\Omega_{ai} + \Omega_{aj})\ /2 \qquad 3.50$$

$$P_{cij} = Z_{cij}\ RT_{cij}/V_{cij} \qquad 3.51$$

$$V_{cij} = \frac{1}{8}\ (V_{ci}^{1/3} + V_{cj}^{1/3})^3 \qquad 3.52$$

$$Z_{cij} = 0.291 - 0.08\ \omega_{ij} \qquad 3.53$$

$$\omega_{ij} = (\omega_i + \omega_j)\ /2 \qquad 3.54$$

These parameters reduce to those of the pure components if $i = j$ in Equation (3.48). It may be mentioned that Equations (3.45 - 3.48) follow the proposals of Redlich and Kwong [10], Equations (3.49 - 3.51), that of Cheuh and Prausnitz [11] and Equations (3.53 - 3.54) that of Pitzer and his coworkers [11]. Equation (3.52) is the well known Lorentz relationship.

In this investigation it is intended to find the value or values of k_{ij} for which the activity coefficient of the solute γ_2, calculated from Equation 3.30 equals that evaluated from Equation 3.32 by means of the Redlich-Kwong equation of state [10] and the mixing rules 3.45 - 3.54. The k_{ij} values determined can, it is hoped, be used, once its dependency on the system temperature T, and pressure P, and the solute mole fraction x_2, is established to predict the solubility at a given temperature and pressure.

CHAPTER 4. EXPERIMENTAL DETERMINATION OF THE SOLUBILITIES OF HEAVY HYDROCARBONS IN LIQUID METHANE

In this chapter, the details of the equilibrium cell and its supporting equipment, the analytical equipment and the materials used in this study will be described. The experimental results will also be presented.

4.1 Equipment

The forced vapour recirculation equipment used was essentially the same as that used by previous researchers (11,14) but with minor changes to the liquid nitrogen line. Formely, liquid nitrogen was being generated in situ by means of a cryogenerator (Phillips model PPG 102) but when this unit developed a fault, changes had to be made to the liquid nitrogen line so that liquid nitrogen in tanks could be used.

A schematic flow diagram of the experimental equipment is shown in Figure 4.1 and detailed diagram of the equilibrium cell in Figure 4.2. The overall equipment consists of the following sections:

i) The feed charging system.

ii) The equilibrium cell.

iii) The recirculation loop.

iv) The sampling system.

v) The cryostat and its temperature controller.

vi) The temperature and pressure measuring devices and the

vii) Analytical system.

i) Feed Charging System

The feed charging system was made up of two or three supply cylinders containing the pure gases and equipped individually with pressure regulators and valves. The valves were used to link the supply cylinders to the feed line to the equilibrium cell. Mixture components were charged into the equilibrium cell in the following manner. First the evacuated equilibrium cell was charged with the solute. Normal butane, the only gaseous solute among the lot studied was charged into the cell directly from the supply cylinder. The liquid solutes (n-pentane, n-hexane, n-octane, n-nonane) were first transferred from their respective reagent bottles into a hypodermic syringe and then injected into the cell through a septum.

When sufficient solute had accumulated in the cell, cooling was continued until the bath temperature was a few degrees above the freezing point of the solute. At this stage the solvent gas (methane) was charged into the cell from its supply cylinder until the cell was about two thirds full of material.

ii) The Equilibrium Cell

This consisted of a 100 ml Jerguson transparent gauge with a stainless steel body. Teflon gaskets

were inserted between the thick glass windows and the metal body. A four inch long, 0.50 inch O.D. stainless steel nipple through which a vapour outlet line and two stainless liquid sampling tubes were inserted at the top of the cell. A vapour inlet line was inserted horizontally into the equilibrium cell about 1.5 inches from the bottom of the cell with its tip extended to the centre of the cell. Two copper constantan thermocouples of 0.0625 inch O.D. together with their protective stainless steel sheaths were also inserted into the cell. One of the thermocouples was placed in the vapour phase the other in the liquid phase. All fittings were made of stainless steel and were tested to withstand the experimental conditions. The details of the equilibrium cell are shown in Figure 4.2.

iii) The Recirculation Loop

The purpose of the recirculation loop is to provide thorough agitation of the cell contents and thus speed up equilibration.

An electromagnetic pump was used to extract some of the vapour phase and recirculate it through the liquid phase by forcing it through a coiled stainless steel tubing, immersed in the bath, which enters the cell horizontally about 1.5 inches from the bottom. The recirculation rate can be adjusted

by varying the speed of the pump. The volume regulator served as a part of the recirculation loop and is used in the regulation of pressure during the liquid sampling period.

iv) Sampling System

In this study only the liquid phase was sampled for analysis. The liquid samples were taken through a stainless steel tube of 0.0625 inch I.D. A needle valve was inserted in the line between the equilibrium cell and the sample bulb in order to minimize the sample size and to control the sampling rate.

v) The Cryostat and Its Temperature Controller

A Dewar flask of 18 litres capacity was used as the cryostat. Unsilvered vertical strips on the opposite sides of the flask allow visual observation of the interior of the bath and cell. The bath is illuminated by a 100 watt lamp mounted behind the rear slit. The cryostat is equipped with two variable speed stirrers, a refrigeration coil and a heating element connected to a proportional type Bayley Precision Temperature controller, model 250, which was used to control the bath temperature.

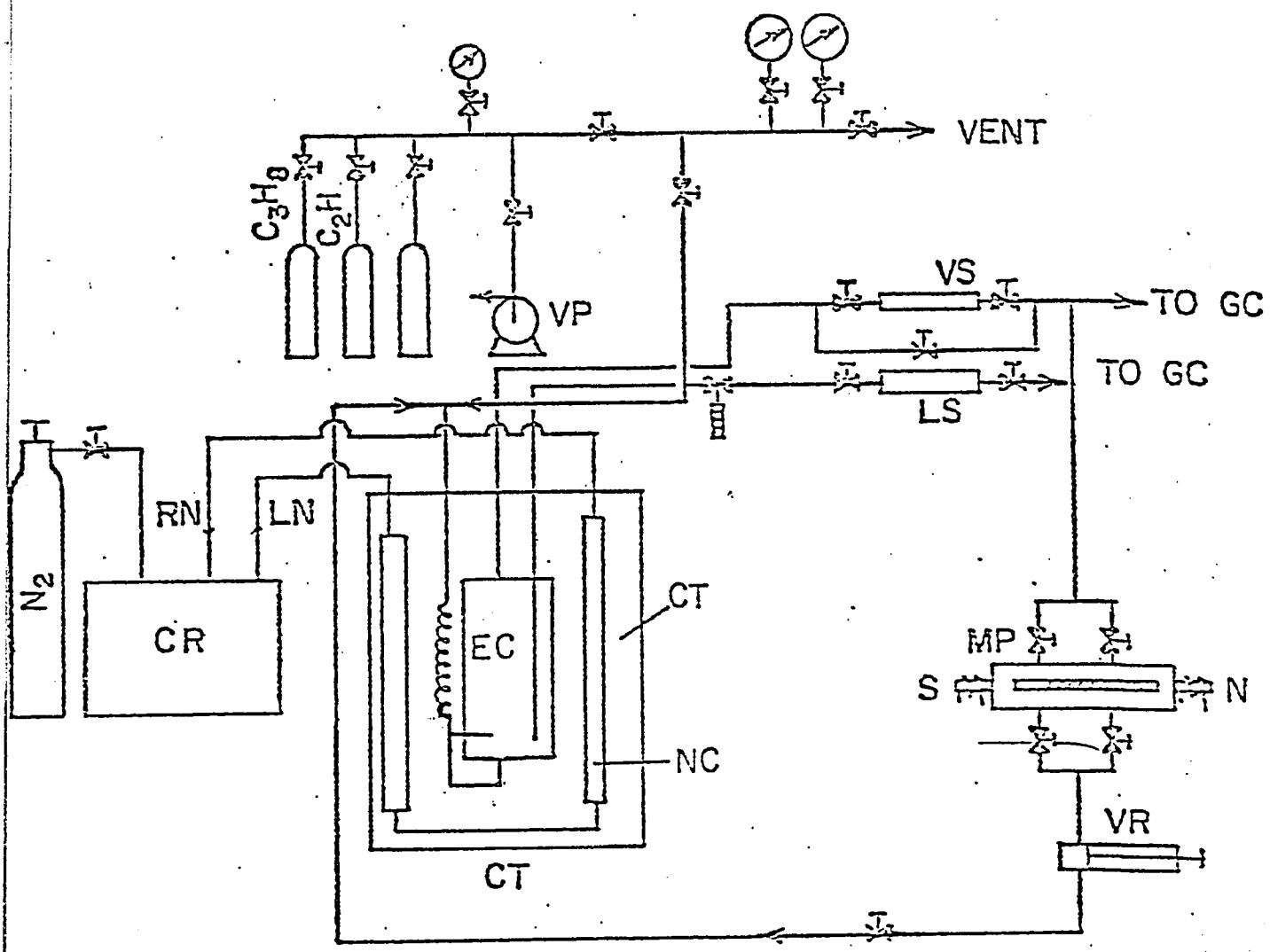

CT	CRYOSTAT	MP	MAGNETIC PUMP
EC	EQUILIBRIUM CELL	NC	NITROGEN VAPORIZATION COIL
CR	PHILIPS CRYOGENIC SYSTEM		
LS	LIQUID SAMPLING BULB	VP	VACUUM PUMP
		VR	VOLUME REGULATOR
		VS	VAPOR SAMPLING BULB
		LN	LIQUID NITROGEN
		RN	RETURN NITROGEN

Figure 4.1 A Schematic Flow Diagram of the Apparatus

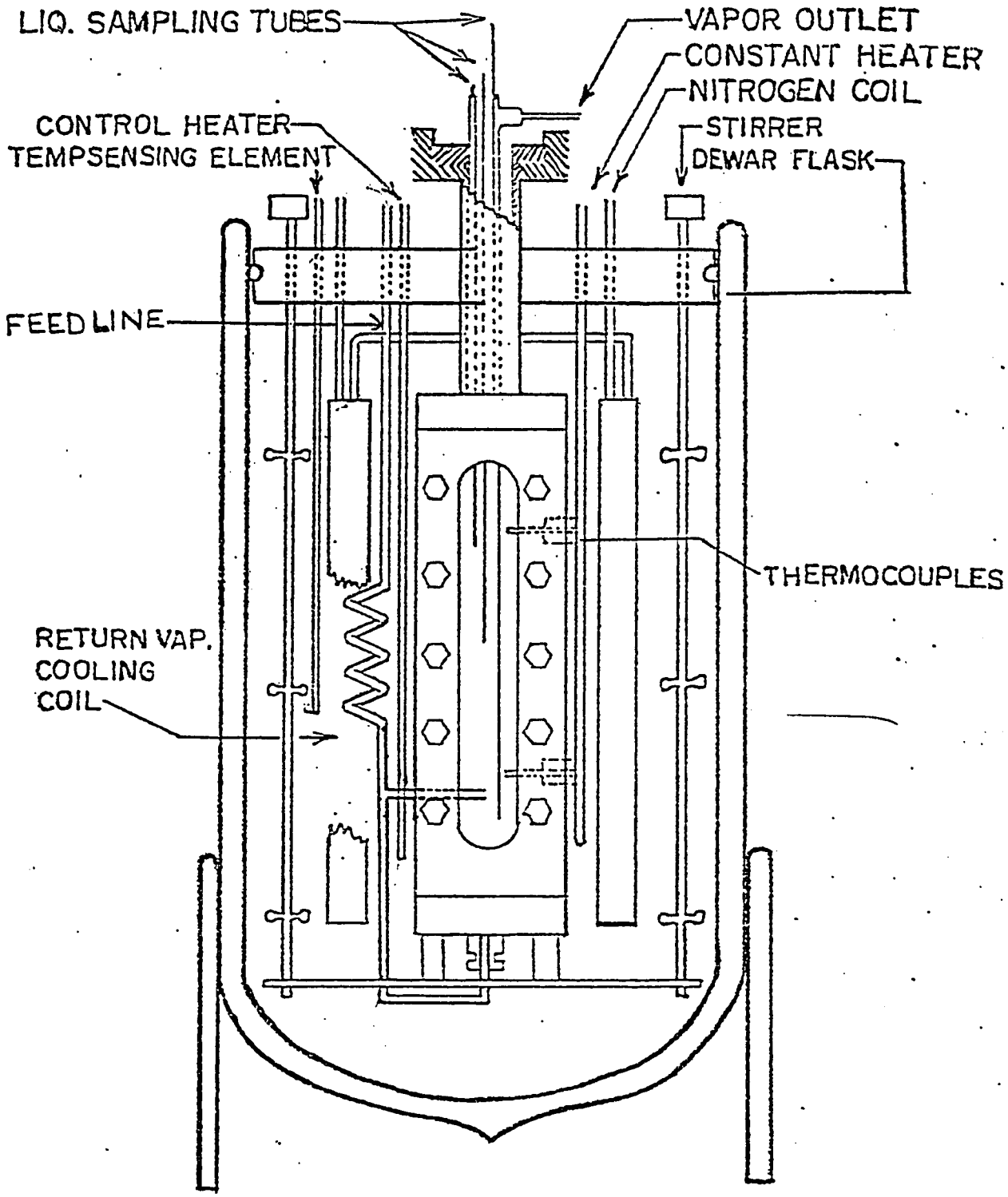

Figure 4.2 The Equilibrium Cell and the Cryostat

The temperature controller is effective in the temperature range - 200°C to +100°C.

Isopentane was used as the bath liquid. The coolant was liquid nitrogen and was forced through the cooling coils from a liquid nitrogen tank by compressed air or by gaseous nitrogen at 20 psig pressure. The temperature of the cryostat was regulated by controlling the evaporation rate of liquid nitrogen in the refrigeration coil and was controlled to $\pm$ 0.01K.

vi) Temperature and Pressure Measuring Devices

System temperatures were measured by means of two copper - constantan thermocouples connected to a Leeds and Northrup K-5 potentiometer. One of the thermocouples was in the vapour phase, the other in the liquid phase. The thermocouples were calibrated against the vapour pressure of methane (15). The pressure in the cell was measured by means of two pretested 12 inch (Heise) Bourdon gauges. The ranges of the two gauges are from 0 to 200 psia and from 0 to 2000 psia with 0.2 and 2 psia per division. The 0 - 200 psia gauge was used when recording pressures in the range 0 - 200 psia while for pressures exceeding 200 psia the 0 - 2000 psia gauge was used. The accuracy of the gauges is 0.1% of the full scale reading.

vii) Analytical System

Analysis of the liquid samples were made with a Hewlett-Packard gas chromatograph Model 5750B, equipped with a flame ionization detector and a Westronics MT21 recorder. The flame ionization detector (FID) has high sensitivity to hydrocarbons and low response to common pollutants such as water vapour, carbon dioxide CO_2, carbon monoxide CO, helium He, argon Ar, and nitrogen N_2.

"Porapak Q" (80 - 100 mesh) was used as the column packing material and the column was 48 inches long with an outside diameter of 0.25 inches.

Helium was chosen as the carrier gas because it has a very low solubility in hydrocarbons especially at low temperatures. It can be obtained commercially with high purity (<0.5 ppm hydrocarbons). It has a very low response in a flame ionization detector.

4.2 Materials

The solvents and solutes were purchased from the suppliers listed in Table 4.1. The purities shown are the manufacturers specifications. They were used in this investigation without any attempt at further purification.

TABLE 4.1

MATERIALS USED IN THIS WORK AND THEIR SUPPLIERS

Material	Supplier	Mole %
Methane	Matheson Co.	99.99
Ethane	"	99.96
Propane	"	99.99
n-Butane	"	99.9
n-Pentane	Phillips Petroleum Co.	99.9
n-Hexane	" "	99.9
n-Octane	" "	99.9
n-Nonane	" "	99.9

4.3 Preparation of Calibration Curves and Experimental Procedure

Prior to the determination of the solubilities the thermocouples were calibrated against the vapour pressure of methane [15] and also calibration curves for the methane-n-butane system were prepared. The procedures used in the preparation of the calibration curves and in the determination of the solubilities are described below.

4.3.1 Calibration of Thermocouples

At room temperature the system was evacuated and purged with methane and maintained under vacuum overnight. The cell was then immersed in the Dewar flask which was almost filled with isopentane. The windows of the equilibrium cell were centred with respect to the vertical unsilvered strips of the Dewar flask.

A 100 watt lamp was used as a source of illumination to ensure clear visibility of the cell and its contents. The flow of liquid nitrogen was started and the bath stirrers turned on at the same time.

After about three hours of cooling when the bath temperature was sufficiently low enough to ensure liquefaction of methane, gaseous methane is fed into the cell until the cell was about half filled with liquid methane.

The temperature controller and electromagnetic pump were activated and kept on until equilibrium was attained. This was indicated by constant pressure and voltage readings on the pressure gauges and the potentiometer. The electromagnetic pump was stopped and the liquid and vapour phases allowed to settle after which the pressure and voltage readings were recorded.

Readings were taken while the bath temperature was being lowered and also while it was being raised.

The vapour pressure versus voltage readings obtained were converted into a voltage versus temperature calibration curve (see Appendix A) using the vapour pressure versus temperature data of Prydz and Goodwin [15].

4.3.2 Preparation of Calibration Curves for the Methane-n-butane System

The procedure adopted for the preparation of the calibration curve is as follows:

(i) Preparation of methane-n-butane mixtures of known compositions.

(ii) Analysis of prepared mixtures and calculation of peak area ratios.

(i) Preparation of Mixtures:

A Pope Porta-Vac high vacuum system capable of evacuating to pressures as low as 10^{-6} torr was

used to evacuate cylindrical (6.0 x 3.5 cms) copper sample containers.

An evacuated container was partly filled with butane and the pressure recorded. Methane was then added and the final total pressure noted. Assuming that the total pressure in a container was equal to the partial pressures of the butane and methane, the mole fractions of the n-butane and methane were computed as the ratio of individual partial pressures to the total pressure.

(ii) Analysis and Calculation of Peak Area Ratios

The prepared mixtures were stirred overnight to homogenize them before being analyzed by the gas chromatograph. An average of ten sample injections into the gas chromatograph were made for each prepared sample. The sample containers were heated by means of electrical heating tape both during the stirring and analysis.

The heating was to ensure that the components of the mixture were properly mixed. Peak area ratios were read from the integrator printout and a plot of peak area ratios versus mole fractions ratios (see Appendix A) prepared. The resulting curves were used to determine mole fraction ratios and subsequently the mole fractions of samples obtained from actual experimental runs.

It was not feasible to prepare calibration curves of peak area ratios versus mole fraction ratios for the solutes n-pentane, n-hexane, n-octane and n-nonane by the partial pressure method outlined above since the solvent is a gas at room temperature and the solutes liquid. As such it was not possible to combine the two together to form a homogeneous mixture of known composition as in the case where both solvent and solute were gases. To obviate this difficulty, Relative Sensitivity Factors for the Hydrogen Flame Detector [16] were used to convert peak areas into true areas.

To convert peak areas obtained from the integrator printout into actual areas, each area is divided by the Relative Sensitivity to get true area. Normalizing the results gives weight percent of each component. Using a basis of 100 pounds weight and the molecular weights of the compounds under study, the percentages by weight are converted into mole fractions. A sample calculation is given in Appendix C.

For hydrocarbons, with two exceptions, the values of the Relative Sensitivities are all approximately 1.0. The two exceptions are benzene 1.12, and toluene 1.07.

The Relative Sensitivities used in this work are listed in Table 4.2.

TABLE 4.2

RELATIVE SENSITIVITY DATA FOR HYDROGEN FLAME DETECTOR

Normal Paraffins	Relative Sensitivity
Methane	0.97[16]
Ethane	0.97
Propane	0.98
Butane	1.09
Pentane	1.04
Hexane	1.03
Octane	0.97
Nonane	0.98

4.3.3 Determination of Solubilities

The determination of the solubilities involved at the following steps:

(i) Charging the equilibrium cell with the components of the system under investigation

(ii) Equilibration

(iii) Sampling and analysis

(i) Charging the components of a mixture into the equilibrium cell

The system was first evacuated, purged with the less volatile component at room temperature, evacuated again and maintained under vacuum overnight.

The Dewar flask was then filled with isopentane and the equilibrium cell immersed completely in it. The windows of the equilibrium cell were centred with respect to the vertical unsilvered strips of the Dewar flask. The flow of liquid nitrogen was started and the bath stirrers turned on soon afterwards.

The equilibrium cell was allowed to cool down for some time and then the heavier component or solute gas charged until sufficient of it has liquefied. When the temperature was a few degrees from the freezing point of the solute the solvent gas was charged into the cell.

The electromagnetic pump and temperature controller were turned on and the bath temperature brought down slowly until the solute starts precipitating out from solution an indication that the solution was saturated at the particular temperature and pressure. Liquid solutes n-pentane, n-hexane, n-octane and n-nonane were injected into the cell through a self sealing septum prior to its immersion in the bath.

(ii) Equilibration

The temperature at which the solute starts to separate out was maintained constant by means of the temperature controller. Vapour recirculation was continued for at least three hours after the appearance of the solid phase. When the potentiometer and pressure gauges were recording constant readings the electromagnetic pump was turned off and the solid particles in suspension allowed to settle.

(iii) Sampling and Analysis

After the solution has settled for about an hour, the pressure and voltage readings were recorded. The sampling system was evacuated before withdrawal of a sample from the cell. The first portion of the liquid sample was totally vaporized to purge the sampling line and also for estimating the sampling rate. The rate was regulated by two valves in series; the first which was adjacent to

the high pressure side was partially open and the second, a needle valve was opened slightly. The collected sample was heated to about 50°C and stirred overnight before being analyzed by the gas chromatograph.

At least ten analyses were made for each of the samples collected and the average peak area ratio calculated.

Further readings were obtained for different temperatures and pressure using the procedure outlined above.

Problems arising from the inability of the circulation pump to deliver adequate outlet pressure at very low temperatures resulted in very poor agitation at these temperatures and this together with solid deposition in the return vapour coil prevented us from continuing our data taking to very low temperatures.

4.4 Experimental Results

Equilibrium pressure (P) - temperature (T) and liquid phase mole fraction (X) measurements were made for the following systems at the conditions specified below:

System	Temperature K	Pressure-Psia
Methane-n-butane	113.3 - 129.0	13.6 - 20.6
Methane-n-pentane	123.4 - 131.3	33.4 - 49.2
Methane-n-hexane	119.1 - 166.2	23.8 - 280.5
Methane-n-Octane	156.3 - 179.7	198.0- 484.6
Methane-n-nonane	161.6 - 184.3	250.0- 588.5
Methane-ethane-n-hexane	114.6 - 154.8	17.6 - 116.4
Methane-propane-n-hexane	120.4 - 153.0	23.0 - 89.

The experimental data are presented in Tables 4.3 to 4.9.

TABLE 4.3

EXPERIMENTAL RESULTS FOR THE BINARY SYSTEM

METHANE(1)-n-BUTANE(2)

Temperature K	Pressure Psia	Mole Fraction x_2
129.0	17.8	0.8115
124.7	20.4	0.6938
123.2	20.6	0.6811
122.6	20.3	0.6460
119.0	18.4	0.5315
117.1	17.4	0.4334
113.3	13.6	0.2830

TABLE 4.4

EXPERIMENTAL RESULTS FOR THE BINARY SYSTEM

METHANE(1)-n-PENTANE(2)

Temperature K	Pressure Psia	Mole Fraction Pentane x_2
131.3	49.15	0.4119
130.2	48.0	0.3866
129.4	47.25	0.2846
128.1	43.8	0.1884
127.8	42.8	0.1585
125.9	38.4	0.0971
123.4	33.4	0.0509

TABLE 4.5

EXPERIMENTAL RESULTS FOR THE BINARY SYSTEM

METHANE(1)-n-HEXANE(2)

Temperature K	Pressure Psia	Mole Fraction Hexane x_2
166.2	280.5	0.1795
161.0	231.0	0.0640
159.6	216.0	0.0409
154.8	182.0	0.0292
149.0	140.4	0.0120
133.4	68.6	0.0044
124.7	38.7	0.0007
119.1	23.8	0.0002

TABLE 4.6

EXPERIMENTAL RESULTS FOR THE BINARY SYSTEM

METHANE(1)-n-OCTANE(2)

Temperature K	Pressure Psia	Mole Fraction Octane x_2
179.7	484.6	0.0064
173.9	398.75	0.0036
166.0	297.0	0.0013
156.3	198.0	0.0004

TABLE 4.7

EXPERIMENTAL RESULTS FOR THE BINARY SYSTEM

METHANE(1)-n-NONANE(2)

Temperature K	Pressure Psia	Mole Fraction Nonane x_2
184.3	588.5	0.0018
181.3	522.0	0.0013
176.3	433.0	0.0010
171.4	363.0	0.0005
161.6	250.0	0.0003

TABLE 4.8

EXPERIMENTAL RESULTS FOR THE TERNARY SYSTEM

METHANE (1)-ETHANE (2)-n-HEXANE (3)

Temperature K	Pressure Psia	Mole Fraction Ethane x_2	Hexane x_3
154.8	116.4	0.4092	0.2039
153.3	124.0	0.2958	0.1670
150.7	104.0	0.3868	0.0626
140.3	82.8	0.2206	0.0225
134.9	57.0	0.2076	0.0082
116.4	22.3	0.1831	0.0036
114.6	17.6	0.1524	0.0018

TABLE 4.9

EXPERIMENTAL RESULTS FOR THE TERNARY SYSTEM

METHANE(1)-PROPANE(2)-n-HEXANE(3)

Temperature K	Pressure Psia	Mole Fraction Propane x_2	Hexane x_3
153.0	89.0	0.4961	0.1578
145.8	85.9	0.4192	0.1341
135.6	56.7	0.3329	0.0448
127.2	38.8	0.1671	0.0141
120.4	23.0	0.1650	0.0065

The experimental data obtained in this investigation are compared with those available in the literature in Figures 4.3 to 4.9.

From Figures 4.3 to 4.5 it is apparent that our data shows good agreement with the data of Kuebler and McKinley at high and moderate solute concentrations. However, at very low temperatures and hence low solute concentrations there is discrepancy.

The data obtained at very low temperatures are unreliable owing to the frequent blockage of the return vapour coil by solids which made efficient agitation of the cell contents extremely difficult.

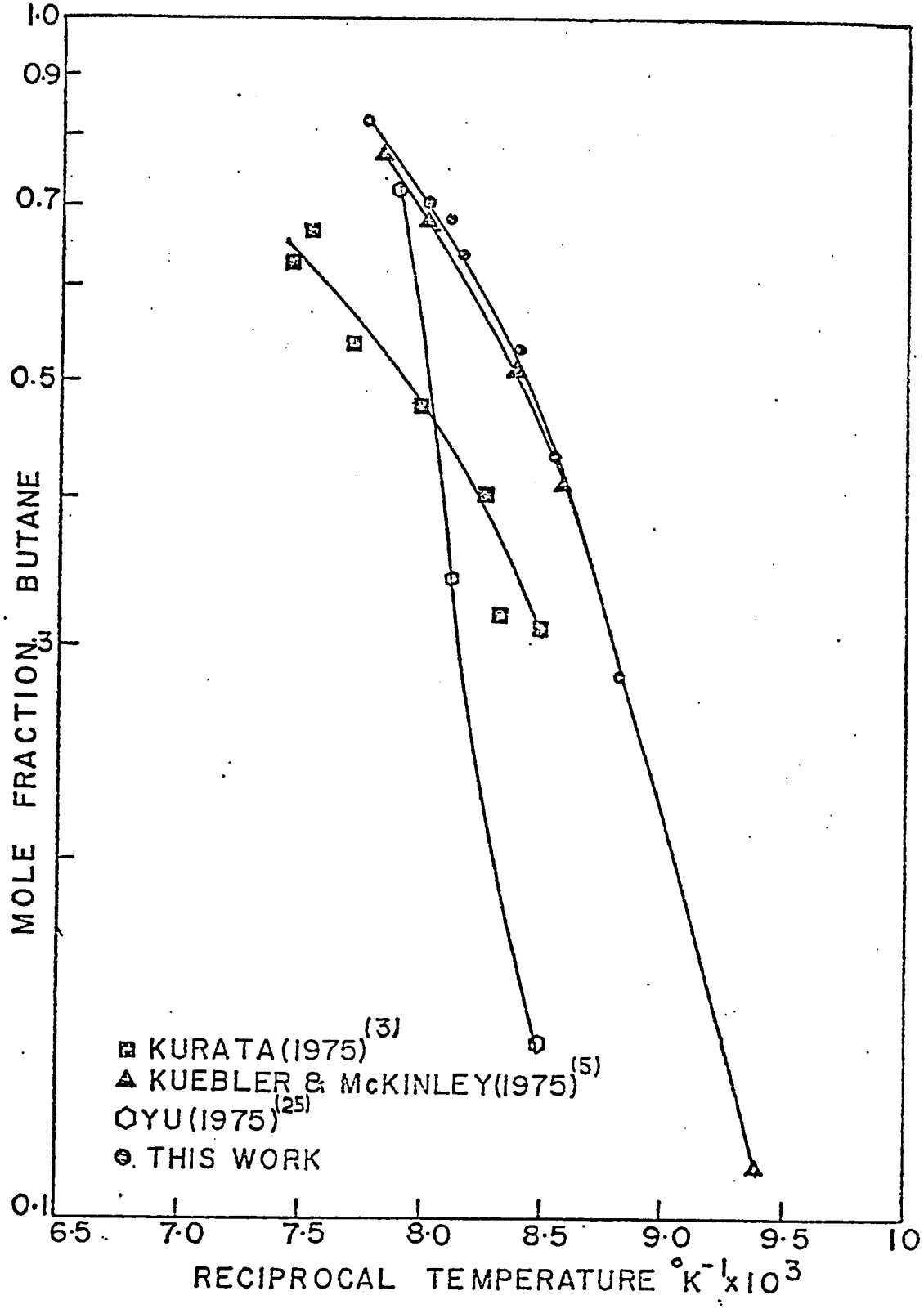

Figure 4.3 A Plot of the Solubility of Solid n-butane in Liquid Methane.

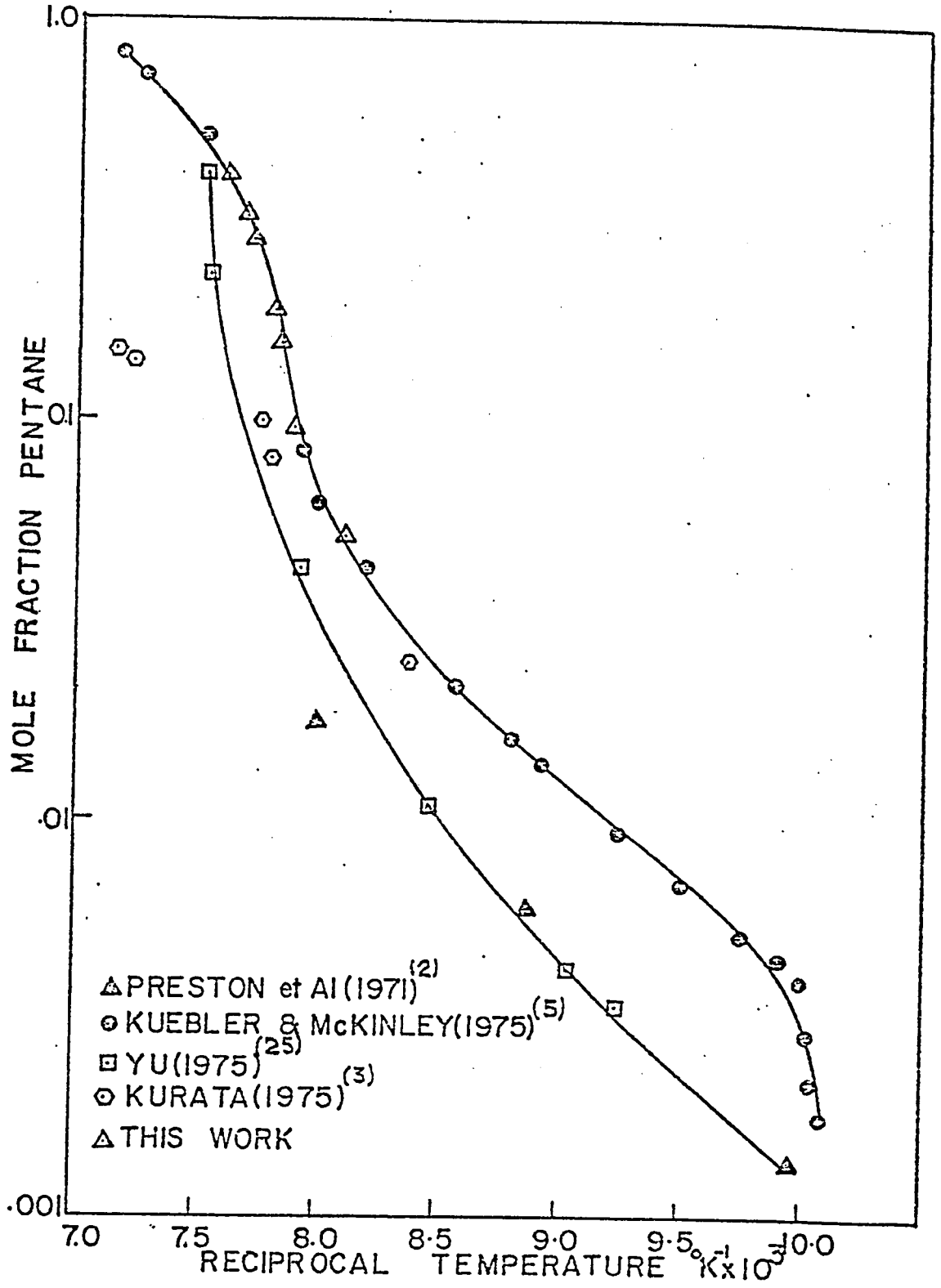

Figure 4.4 A Plot of the Solubility of Solid n-pentane in Liquid Methane.

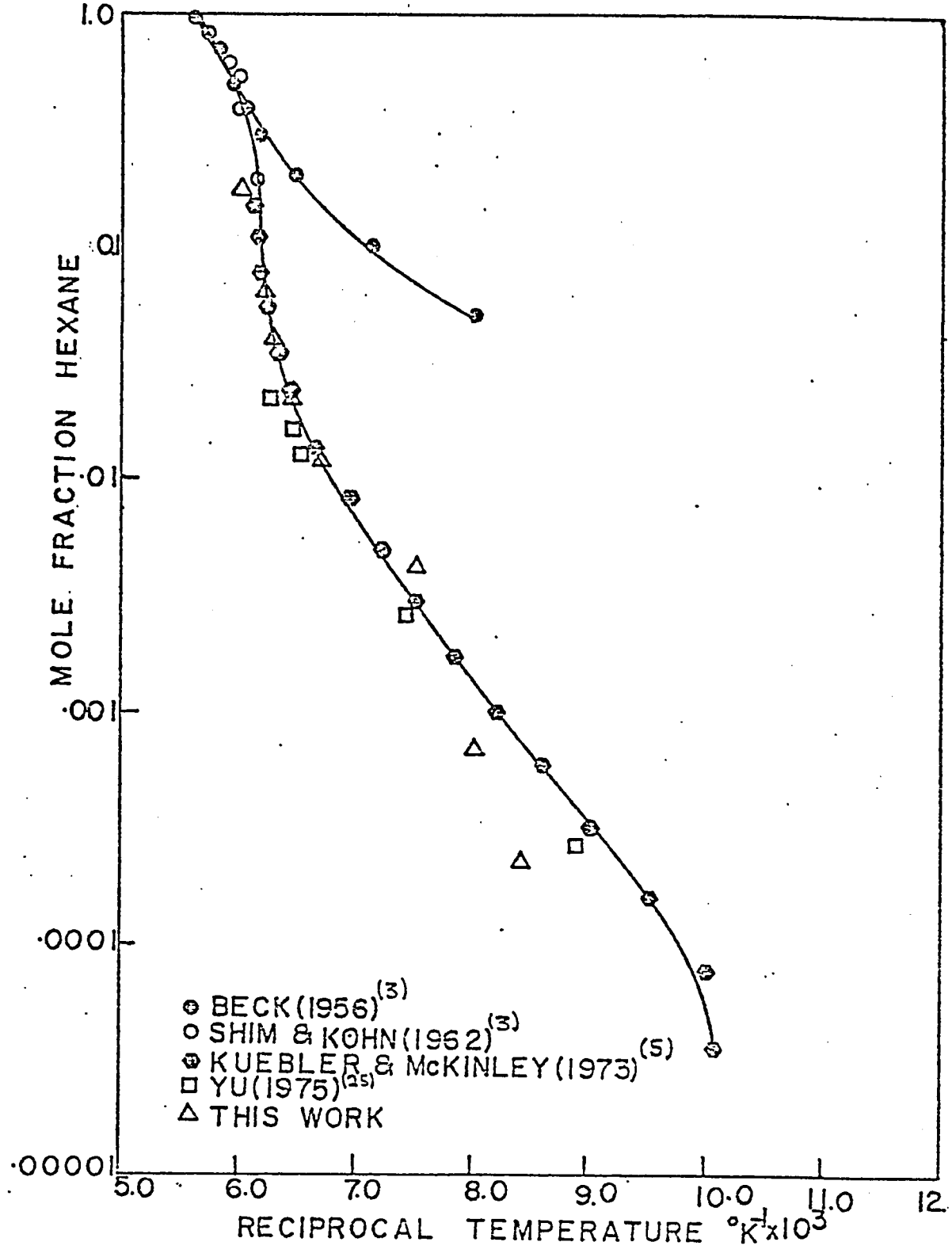

Figure 4.5 A Plot of the Solubility of Solid n-hexane in Liquid Methane.

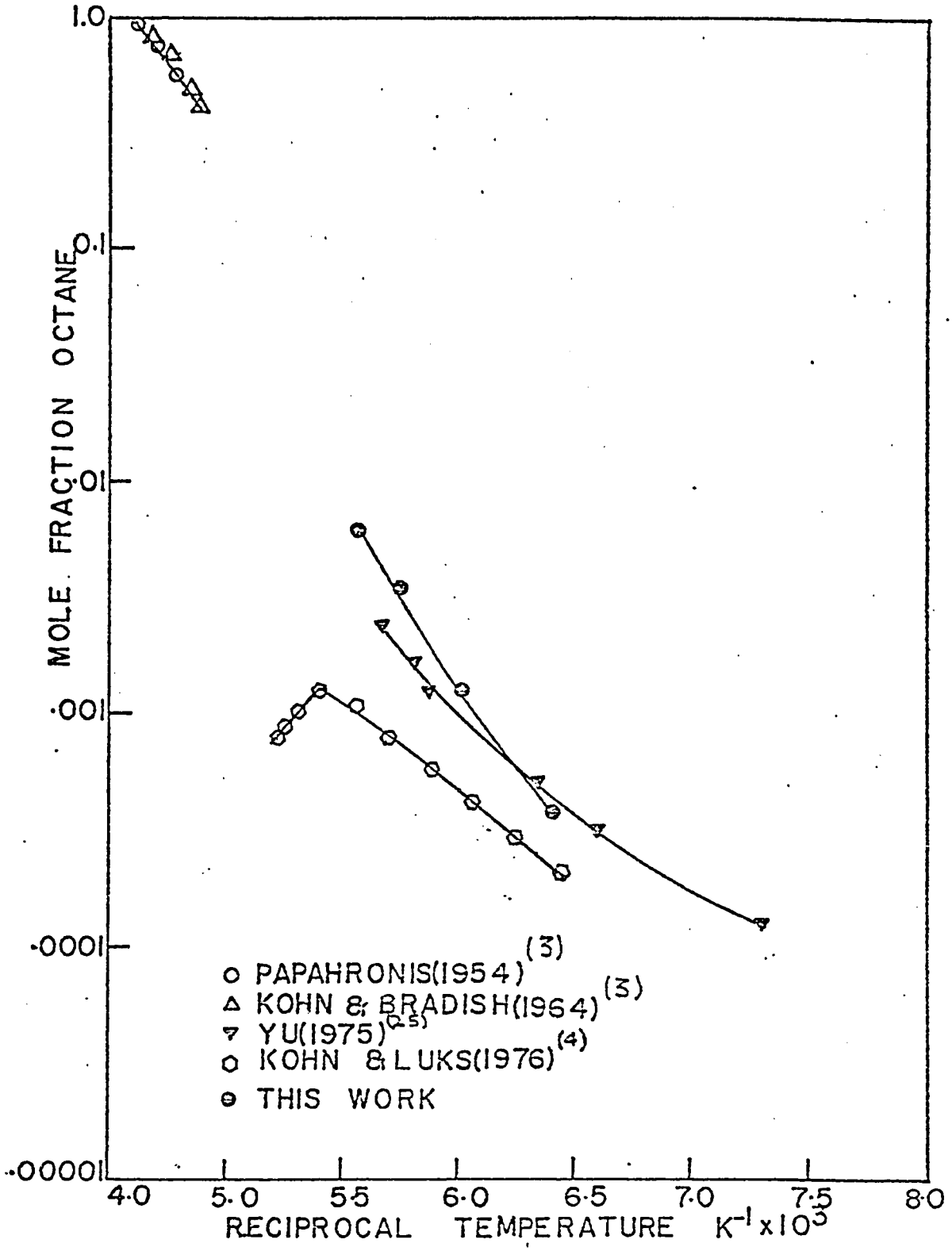

Figure 4.6 A Plot of the Solubility of Solid n-octane in Liquid Methane.

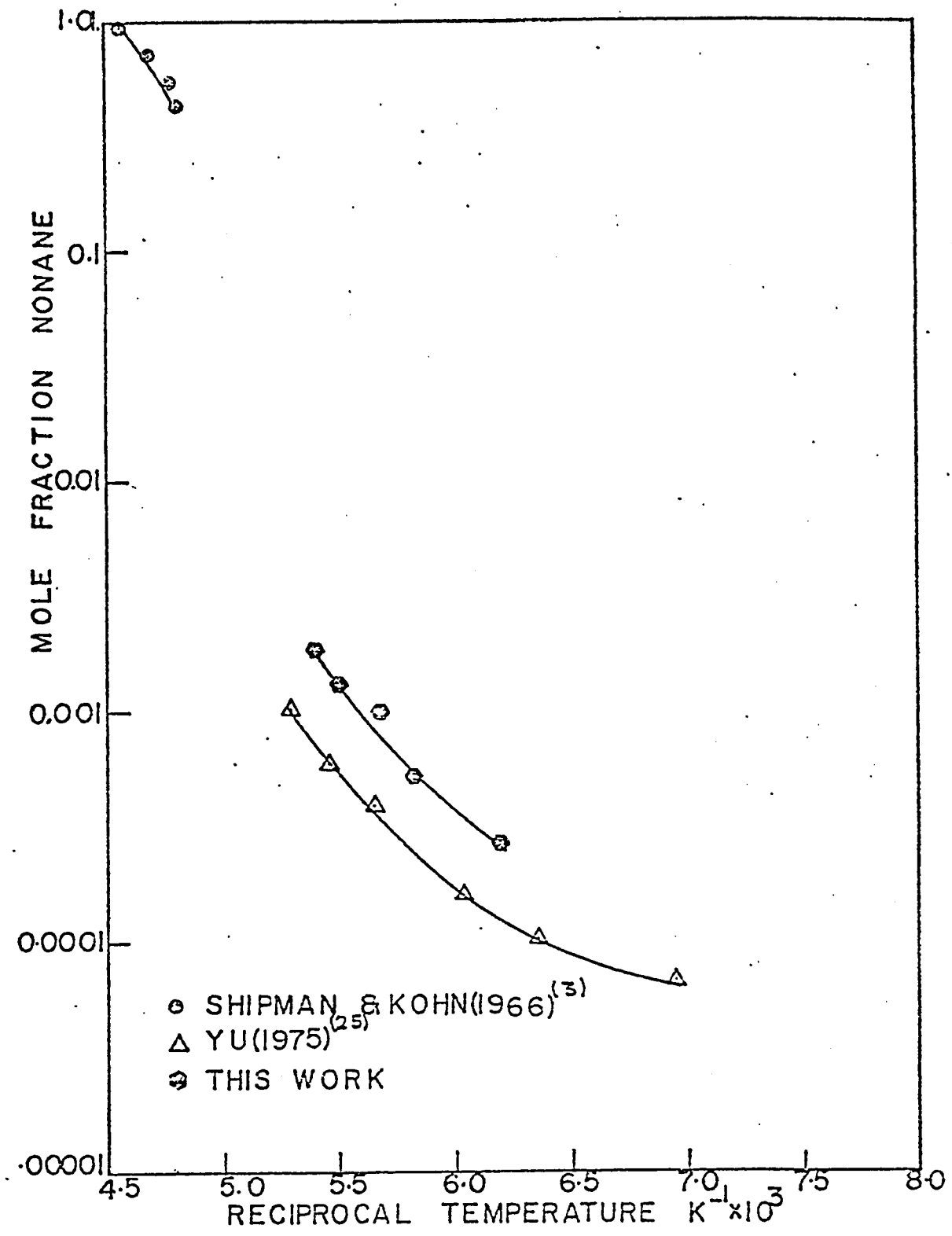

Figure 4.7 A Plot of the Solubility of Solid n-nonane in Liquid Methane.

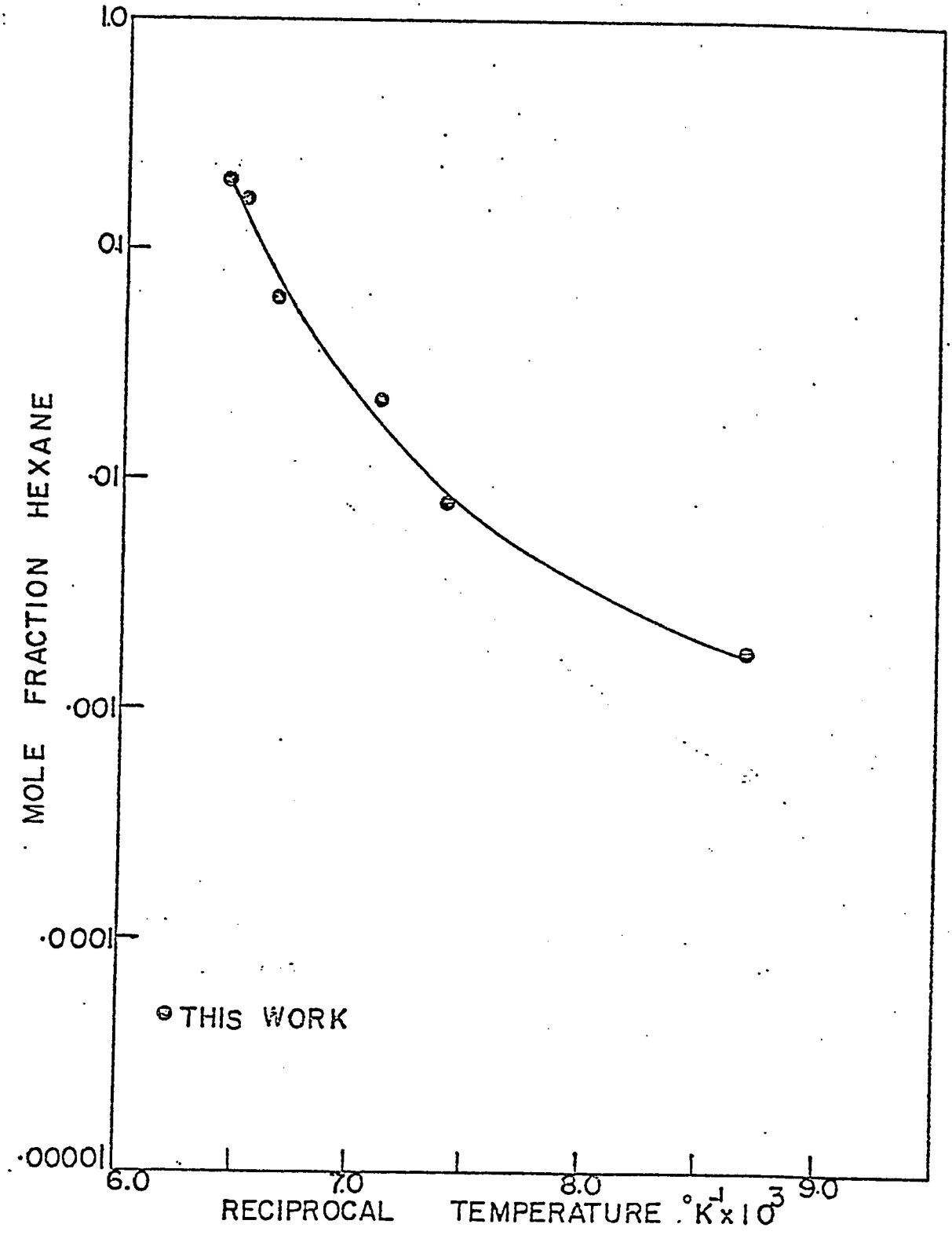

Figure 4.8 A Plot of the Solubility of Solid n-hexane in the Mixed Solvents of Methane and Ethane.

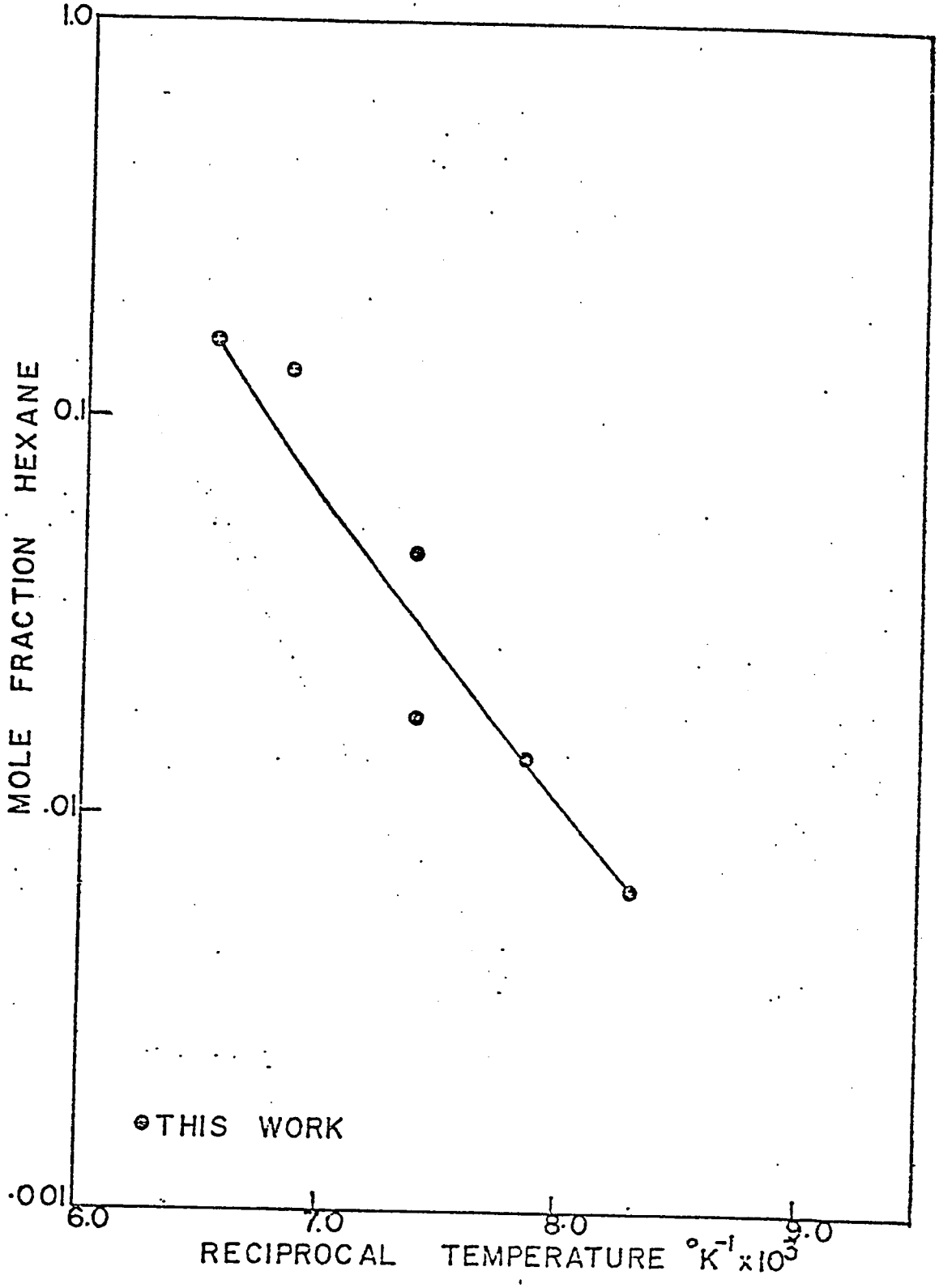

Figure 4.9 A Plot of the Solubility of Solid n-hexane in the Mixed Solvents of Methane and Propane.

4.5 Experimental Errors

Possible sources of error are the pressure gauges, the potentiometer and the gas chromatograph. The pressure and temperature errors could be estimated. The concentration error is however difficult to estimate. It will not be substantial since the use of the electronic integrator gives very accurate peak areas so errors arising from peak tailing are significantly minimized. The total concentration error is estimated to lie in the range 0.001 to 0.005 mole fraction. This error was minimized by repeated analyses and by using average values in the calculation. (See appendix D for sample calculation.)

Temperature Error:

The temperature of the cryostat was controllable to 0.01K and the temperatures measured were probably accurate to $\pm$ 0.1K.

Pressure Error:

The accuracy of the Heise gauges is 0.1% of the full scale deviation. For pressures up to 200 psia, the error is 0.2 psia; for higher pressures the 2000 psia was used to give an error of 2 psia. At the lowest experimental pressure of 13.6 psia the relative error is 1.5% while at the highest experimental pressure of 588.5 psia it is about 0.33%.

CHAPTER 5. CORRELATION OF EXPERIMENTAL RESULTS

In Chapter 3, it was shown that for ideal solubility the plot of ℓnx versus 1/T is a straight line of slope $\frac{\Delta S_f}{R}$. Since the solubility plots Figures 4.3 to 4.7 all deviate from a straight line, the solubilities are non-ideal and are therefore described by Equation (3.31).

$$\ell n\ \gamma_2\ x_2 = \frac{\Delta S_f}{R}\ (1 - \frac{T_f}{T}) \qquad 3.30$$

The method used to correlate our results was to evaluate the activity coefficient of the solute γ_2 using Equation (3.31) and Equation (3.33), the Redlich and Kwong equation of state and the proposed mixing rules stated in Chapter 3.

The objective of the correlation attempt was the determination of the value of the binary interaction constant k_{ij} for which the activity coefficient of the solute γ_2, calculated from Equation (3.30) equals or agrees, within a specified limit, with that calculated by means of the Redlich-Kwong Equation of state.

From Equation (3.30) it is apparent that the activity coefficient of the solute γ_2, can be evaluated without much difficulty since the quantities ΔS_f, T_f, T and x_2 are known.

From Equation (3.32),

$$\gamma_{i\ell} = \frac{f_{i\ell}\ (P, T, x)}{x_i\ f^{\circ}_{i\ell}\ (P, T)} \qquad 3.32$$

the quantities $f_{i\ell}$ (P, T, x) and $f^{\circ}_{i\ell}$ (P, T) must be evaluated by means of an equation of state.

The solid-liquid equilibrium may be described mathematically by the equation

$$\hat{f}_2 = f^{s}_{2s} = \gamma_2 \, x_2 \, f_{2\ell} \qquad 5.1$$

where $\hat{f}_2$ is the solubility of the solute in solution.

Equation (5.1) may be rearranged to give

$$\gamma_2 \, x_2 = \frac{\hat{f}_2}{f_{2\ell}} = \frac{f_{2s}}{f_{2\ell}} = \left(\frac{\hat{f}_2}{P \, x_2}\right) \left(\frac{P}{f_{2\ell}}\right) x_2 \qquad 5.2$$

$$\therefore \gamma_2 \, x_2 = \left(\frac{\hat{f}_2}{P \, x_2}\right) \left(\frac{P}{f_{2\ell}}\right) x_2 \qquad 5.3$$

or $$\gamma_2 = \hat{\phi}_{2\ell} \; \frac{P}{f_{2\ell}} \qquad 5.4$$

where $$\hat{\phi}_{2\ell} = \hat{f}_{2/P} \, x_2$$

The quantity $f_{2\ell}$ is the fugacity of the pure subcooled liquid solute at the temperature T, and pressure P, of the system. It can be evaluated by means of the following equation [7]

$$\ell n \; (f/P)_{\text{pure } i} = \int_0^P \frac{(Z_i - 1)}{P} \, dP \qquad 5.5$$

where Z, the compressibility factor is defined by

$$Z = \frac{PV}{RT} \qquad 5.6$$

Using the Redlich-Kwong Equation, the integrated form of equation (5.5) can be expressed as [7]

$$\ell n \left(\frac{f}{P}\right)_{\text{pure } i} = (Z - 1) - \ell n \, (Z - \frac{bP}{RT}) - \frac{a}{bRT^{1.5}} \, \ell n \left(1 + \frac{bP}{ZRT}\right) \qquad 5.7$$

Equation (5.7) [7] is used to evaluate the fugacity of the subcooled liquid at the temperature T and saturation pressure P^{sat}.

To account for the compression of the subcooled liquid from the saturation pressure P^{sat} to the system pressure P, the exponential correction (often called the Poynting Correction) will be used.

In general, the volume of a liquid or a solid is a function of both temperature and pressure, but at conditions remote from critical, a condensed phase may often be regarded as imcompressible and in that case the Poynting correction takes the simple form

$$\exp \frac{V_i^c \ (P - P_i^{sat})}{RT} \qquad 5.8$$

where V_i^c is the volume of the condensed phase which in this case is the subcooled liquid.

The ratio $(f/p)_{pure\ i}$ is the fugacity coefficient of the pure component i. When i is a component of a mixture the fugacity coefficient now becomes $(f_i/x_i P)$ and is expressed for the solute as

$$\ln \left(\frac{f_2}{x_2 P}\right) = (Z-1)\frac{b_2}{b_{mix}} - \ln (Z - b_{mix}P) - \frac{a_{mix}}{b_{mix}RT^{1.5}} \left(\frac{2x_2 a_2 + 2x_1 a_{12}}{a_{mix}} - \frac{b_2}{b_{mix}}\right) \times \ln \left(1 + \frac{b_{mix}P}{ZRT}\right) \qquad 5.9$$

In Equation (5.9), Z is the minimum root of the Equation (5.10) [10]

$$Z^3 - Z^2 + BP\left(A^2/B - 1 - BP\right) Z - \frac{A^2}{B}(BP)^2 = 0 \qquad 5.10$$

$$\text{where } A^2 = a/R^2T^{2.5} = \Omega_a T_c^{2.5}/P_c T^{2.5} \qquad 5.11$$

$$B = \frac{b}{RT} = \Omega_b T_c/P_c T \qquad 5.12$$

5.1 Evaluation of the Temperature Dependent Parameters Ω_a, Ω_b of the Redlich-Kwong Equation of State

It is now generally accepted that the two parameters of the Redlich-Kwong equation, Ω_a, Ω_b, are not universal constants. They vary from substance to substance and are temperature dependent [14]. In this investigation they were evaluated for each substance at the system temperatures studied.

The two parameters Ω_a, Ω_b, can be evaluated from any two pure-component properties at saturation. From vapour liquid equilibrium studies it has been found that the vapour pressure and the saturated liquid volume are the two desirable properties for the evaluation of the two parameters.

Since the solute in solid-liquid equilibrium is a subcooled liquid, no experimental data are available. For this reason we had to rely on extrapolations of generalized correlations. The correlations used in this work were selected among those available by considering the range of reduced temperatures used in the preparation of these correlations. For vapour pressure the correlation of Carruth and Kobayashi [17] was selected and for the molar volume of the

subcooled liquid, the Gunn and Yamada [18] correlation for molar volumes of saturated liquids was used.

The estimated values of the vapour pressures and the corresponding subcooled liquid volumes were used together with the Redlich-Kwong equation of state to calculate the values of the temperature dependent parameters Ω_a and Ω_b of the Redlich-Kwong equation of state.

The smoothed vapour pressure equation of Carruth and Kobayashi [17] together with its constants are listed in Table 5.1.

The Gunn-Yamada correlation [18] for saturated liquid volumes has the following form linear in the acentric factor,

$$V^{\ell}/V_{sc} = V_R^{(0)} \ (1.0 - \omega\delta) \qquad 5.13$$

The generalized functions $V_R^{(0)}$ and δ which are dependent only upon the reduced temperature are tabulated in Table 5.2.

The quantity V_{sc}, is referred to as the scaling volume. It is used in equation (5.13) rather than the critical volume because it is widely recognized that the experimental determination of critical volumes is subject to rather large errors. For this reason the parameter V_{sc} is based on liquid densities which can generally be measured with high accuracy far from the critical point. Table 5.3 lists scaling volumes for a number of compounds.

TABLE 5.1

CONSTANTS OF VAPOR PRESSURE EQUATION[17]

Compound	A	B
C_2H_6	18.0072	- 2049.35
C_3H_8	18.6597	- 2697.80
n- C_4H_{10}	18.8991	- 3246.02
n- C_5H_{12}	19.7269	- 3883.66
n- C_6H_{14}	19.5553	- 4292.80
n- C_7H_{16}	20.1590	- 4852.65
n- C_8H_{18}	20.3621	- 5294.36
n- C_9H_{20}	20.8468	- 5811.26
n- $C_{10}H_{22}$	20.8865	- 6170.32

smoothed vapour pressure equation

$\ell nP = A + B/T$, T in K, P in mm Hg.

TABLE 5.2

REDUCED VOLUME FUNCTIONS FOR NONPOLAR FLUIDS[18]

T_R	$V_R^{(0)}$	δ	T_R	$V_R^{(0)}$	δ
0.20	0.3113	0.2760	0.90	0.5289	0.1754
0.30	0.3252	0.2646	0.92	0.5501	0.1719
0.40	0.3421	0.2521	0.94	0.5771	0.1683
0.50	0.3625	0.2387	0.95	0.5941	0.1664
0.60	0.3862	0.2244	0.96	0.6147	0.1646
0.70	0.4157	0.2090	0.97	0.6410	0.1628
0.75	0.4341	0.2010	0.98	0.6771	0.1609
0.80	0.4562	0.1927	0.99	0.7348	0.1591
0.85	0.4883	0.1842	1.00	1.000	0

TABLE 5.3

SCALING VOLUMES AND CRITICAL VOLUMES FOR HYDROCARBONS[18]

Compound	V_{sc} cu. cm./g. mole	V_c cu. cm./g. mole
Methane	99.10	99.0
Ethane	145.42	148.0
Propane	199.79	203.0
n-Butane	254.07	255.0
n-Pentane	310.97	304.0
n-Hexane	368.48	370.0
n-Heptane	429.28	432.0
n-Octane	490.30	492.0

The scaling volume is defined by the following relationship:

$$V_{sc} = \frac{V_{0.6}}{0.3862 - 0.0866\omega} \qquad 5.14$$

The quantity $V_{0.6}$ is the molar volume of the liquid at a reduced temperature of 0.6. For compounds not listed in Table 5.3 the definition may be used to evaluate V_{sc}, provided that the critical temperature, the acentric factor, and the liquid density at $T_r = 0.6$ are known.

The method used to evaluate the temperature dependent parameters Ω_a and Ω_b of the Redlich-Kwong equation was that developed by Kato et al. [19]. A brief description of the method is presented here.

One of the drawbacks of the Redlich-Kwong equation is its unrealistic behaviour at the critical point. It is characterized by the conditions that $Z_c = 1/3$, $\Omega_a^\circ = 0.42748$ and $\Omega_b^\circ = 0.08664$. These Ω values are obtained to satisfy the condition of three equal roots at the critical point. However all substances we deal with have Z_c values lower than 1/3, and these two Ω values never lie on the curves for these two parameters derived from experimental data.

In order to avoid this critical anomaly, Kato et al. [19] proposed that apparent critical temperature and pressure, T_c^* and P_c^*, be considered as the pure-component parameters of the Redlich-Kwong equation of state. The proposed parameters are related to the quantities Ω_a and Ω_b of the pure component i as follows:

$$\left.\begin{aligned} \Omega_{ai} &= \Omega_a^{\circ} \left(\frac{T_c^*}{T_c}\right)^{2.5} \left(\frac{P_c}{P_c^*}\right) \\ \Omega_{bi} &= \Omega_b^{\circ} \left(\frac{T_c^*}{T_c}\right)\left(\frac{P_c}{P_c^*}\right) \end{aligned}\right\} \qquad 5.15$$

At a given temperature, the pure component parameters T_c^* and P_c^* are determined so as to make the calculated saturated liquid density equal to the experimentally determined value, and at the same time equalize the fugacity coefficients of the two phases at the vapour pressure.

The Redlich-Kwong equation of state was used in the following form:

$$Z^3 - Z^2 + (A - B - B^2)\, Z - AB = 0 \qquad 5.16$$

where

$$A = \Omega_a^{\circ} \left(\frac{T_c^*}{T}\right)^{2.5} \left(\frac{P}{P_c^*}\right) \qquad 5.17$$

$$B = \Omega_b^{\circ} \left(\frac{T_c^*}{T}\right) \left(\frac{P}{P_c^*}\right) \qquad 5.18$$

According to the conditions stated above, one of the roots of Equation (5.16) must be identical to Z_L, therefore

$$Z_L^3 - Z_L^2 + (A - B - B^2)\, Z_L - AB = 0 \qquad 5.19$$

where $Z_L = \dfrac{PV_L}{RT}$ 5.20

combining equations (5.17) and (5.18) gives

$$\frac{A}{B} = \left(\frac{\Omega_a^{\circ}}{\Omega_b^{\circ}}\right)\left(\frac{T_c^*}{T}\right)^{1.5} \qquad 5.21$$

subtracting equation (5.19) from (5.16) we get

$$Z^3 - Z_L^3 - Z^2 + Z_L^2 + (A - B - B^2)\,(Z - Z_L) = 0 \qquad 5.22$$

Equation (5.22) may be simplified as follows:

$$(Z - Z_L)^3 = Z^3 - 3Z^2Z_L + 3ZZ_L^2 - Z_L^3 \qquad 5.23$$

$$\therefore (Z^3 - Z_L^3) = (Z - Z_L)^3 - 3ZZ_L^2 + 3Z^2Z_L \qquad 5.24$$

$$= (Z - Z_L)(Z^2 + ZZ_L + Z_L^2) \qquad 5.25$$

Substituting for $(Z^3 - Z_L^3)$ in Equation (5.22) using the right hand side (R.H.S.) expression of Equation (5.25), we get

$$(Z - Z_L)(Z^2 + ZZ_L + Z_L^2) - (Z^2 - Z_L^2) + (A - B - B^2)(Z - Z_L) = 0 \qquad 5.26$$

$$(Z - Z_L)\left[Z^2 + ZZ_L + Z_L^2 - Z - Z_L + (A - B - B^2)\right] = 0 \qquad 5.27$$

$$(Z - Z_L)\left[Z^2 - (1 - Z_L)Z - (1 - Z_L)Z_L + (A - B - B^2)\right] = 0 \qquad 5.28$$

$$(Z - Z_L)\left[Z^2 - (1 - Z_L)Z - \{(1 - Z_L)Z_L - (A - B - B^2)\}\right] = 0 \qquad 5.29$$

Since the other two roots of Equation (5.16) are different from Z_L for temperatures and pressures removed from the critical point, $(Z - Z_L)$ will not be equal to zero. Therefore

$$Z^2 - (1 - Z_L)Z - \{Z_L(1 - Z_L) - (A - B - B^2)\} = 0 \qquad 5.30$$

The fugacity coefficient ϕ is evaluated using Equation[19] (5.31).

$$\ln \phi = (Z - 1) - \ln Z - \ln (1 - B/Z) - (A/B) \ln (1 + B/Z) \qquad 5.31$$

Using these equations, the procedure for evaluating the T_c^* and P_c^* at a given temperature is as follows:

1. For the first iteration, T_c^* is assumed to be equal to the critical temperature of the pure component, T_c.

2. Using Equations (5.19) and (5.21) and the value of Z_L evaluated using the estimated subcooled liquid volume and vapour pressure calculate the numerical value of B. If no real roots of B exist from the quadratic equation, multiply the previous value of T_c^* by the factor 1.0001 until two real roots are obtained. Using Equations (5.18) and (5.21) and these roots, P_c^* and A are evaluated.

3. Substitute the computed values of A and B in Equation (5.30) and solve for the other two roots of Equation (5.16). From thermodynamic considerations these two other values of Z must be greater than Z_L. Using this criterion, a reasonable set of roots is selected. The larger root is considered to be Z_v. When no real roots are obtained, the present value of T_c^* is multiplied by the factor 1.0001 and the calculations repeated from step 2.

4. Evaluate fugacity coefficients for the vapour and liquid phase ϕ_v and ϕ_L respectively using equation (5.31) and the values of Z_v and Z_L. Obtain the difference between the fugacity coefficients ($\Delta \ln \phi = \ln \phi_v - \ln \phi_\ell$).

5. It is not probable that in the first iteration $\Delta \ln \phi$ will be equal to 0. If this is the case ie. $\Delta \ln \phi \neq 0$. the value of T_c^* is multiplied by 1.0001 and the calculations repeated commencing from step 2.

Subsequently, the value of T_c^* is changed by a linear approximation on a $\ell n\ \phi$ vs T_c^* plot. An iteration loop is thus built up until the change of T_c^* value is less than the specified tolerance ($|\Delta\ T_c^*| < 10^{-4}$). The final value of P_c^* is then obtained from this acceptable T_c^* in the step 2 of the iteration procedure.

The T_c^* and P_c^* values thus obtained are used to evaluate Ω_a and Ω_b using the Equations (5.14) and (5.15). The estimated values of the vapour pressures, subcooled liquid volumes and calculated values of Ω_a and Ω_b are tabulated in Table 5.4.

The computer program for performing the calculations is listed in Appendix B.

TABLE 5.4

SYSTEM TEMPERATURE T, VAPOUR PRESSURES P° SUBCOOLED LIQUID VOLUMES V_ℓ, AND THE TEMPERATURE DEPENDENT PARAMETERS Ω_a, Ω_b, OF THE REDLICH-KWONG EQUATION FOR PURE HYDROCARBONS

Temperature T°K	Vapour Pressure P° mm Hg.	Saturated Liquid Volume V_ℓ cc/g. mole	Ω_a	Ω_b
	n-Butane			
129.0	1.904×10^{-3}	78.553	0.38804	0.07845
124.7	7.994×10^{-4}	78.1722	0.38397	0.078322
123.2	5.823×10^{-4}	78.0437	0.38260	0.07828
122.6	5.119×10^{-4}	77.9939	0.38201	0.07826
119.0	2.298×10^{-4}	77.7113	0.37838	0.07818
117.1	1.476×10^{-4}	77.5588	0.37615	0.07813
113.3	5.826×10^{-5}	77.2523	0.37186	0.07803
	n-Pentane			
131.25	5.21×10^{-5}	93.5340	0.38994	0.07589
130.2	4.10×10^{-5}	93.4394	0.38897	0.07587
129.4	3.411×10^{-5}	93.3763	0.38831	0.07585
128.1	2.515×10^{-5}	93.2527	0.38712	0.07581
127.8	2.343×10^{-5}	93.2212	0.38703	0.07580
125.9	1.481×10^{-5}	93.0636	0.38473	0.07576
123.4	7.93×10^{-6}	92.8745	0.38246	0.07572
	n-Hexane			
166.2	1.885×10^{-3}	112.0420	0.40966	0.07429
161.0	8.46×10^{-4}	111.4173	0.40509	0.07410
159.6	6.48×10^{-4}	111.2706	0.40479	0.07407
154.8	2.81×10^{-4}	110.7520	0.40116	0.07394

TABLE 5.4 (Cont'd)

Temperature $T^{\circ}K$	Vapour Pressure P° mm Hg	Saturated Liquid Volume V^{ℓ} cc/g. mole	Ω_a	Ω_b
149.0	9.56×10^{-5}	110.1249	0.39640	0.07376
133.4	3.26×10^{-6}	108.6371	0.38261	0.07338
124.7	3.48×10^{-7}	107.8857	0.37406	0.07320
119.1	6.91×10^{-8}	107.4678	0.36827	0.07312
	n-Octane			
179.7	1.12×10^{-4}	144.0145	0.42102	0.07097
173.9	4.18×10^{-5}	143.2793	0.41711	0.07081
166.0	9.81×10^{-6}	142.2499	0.41117	0.07056
156.3	1.36×10^{-6}	141.1093	0.40342	0.07030
	n-Nonane			
184.3	2.29×10^{-5}	159.9363	0.42931	0.06970
181.3	1.36×10^{-5}	159.5454	0.42731	0.06962
176.3	5.47×10^{-6}	158.8292	0.42371	0.06946
171.4	2.13×10^{-6}	158.2034	0.42017	0.06933
161.6	2.73×10^{-6}	156.9696	0.41247	0.06907

5.2 Calculation of the Activity Coefficient of the Solute γ_2

The procedure used to calculate the liquid phase activity coefficient of the solute γ_2 is as described below.

1. For given values of Ω_{ai}, Ω_{bi}, T_{ci}, P_{ci}, V_{ci}, ω_i, P_{2vap}, $V_{2\ell}$, x_2, P, T, T_f, ΔS_f and R, calculate a_i, and b_i from Equations (3.49) and (3.48).
2. Calculate B_i and A_i^2 from Equations (3.42) and (3.41).
3. Calculate γ_2 from Equation (3.31).
4. Calculate Z_L for the pure subcooled liquid from Equation (5.6).
5. Calculate fugacity of pure subcooled liquid $f_{2\ell}^{satd}$ at the system temperature T and at subcooled liquid vapour pressure $P_{2\ell}^{sat}$ using Equation (5.7).
6. Correct the fugacity evaluated in step 5 to system pressure by means of the Poynting correction, Equation (5.8).
7. For a given value of k_{ij}, calculate k_{ij}, A_{ij}, P_{cij}, V_{cij}, Ω_{aij}, ω_{ij}, Z_{cij} from Equations (3.49) to (3.55).
8. Calculate $a_{mixture}$ and $b_{mixture}$ from Equations (3.46) and (3.47).
9. Calculate $B_{mixture}$ and $A^2_{mixture}$ from Equations (5.11) and (5.12).
10. Calculate the coefficients of the cubic Equation (5.10).

11. Solve the cubic Equation (5.10) and take the minimum root as Z_L for the solution.

12. Calculate the liquid phase fugacity coefficient $\left(f_{2/x_2P}\right)$ from Equation (5.9).

13. Calculate γ_2 from Equation (5.3) and compare with that calculated from step 3. If they disagree, assume a new value for k_{ij} and repeat the calculations from step 7. An iteration loop is thus built up until the difference between the two γ_2 values is less than the specified tolerance. The tolerance used in this work is 0.001. A computer program for performing the calculation is listed in Appendix B.

In this work, k_{ij} values were evaluated using the procedure outlined above at the experimental conditions for all the binary systems studied. In addition, k_{ij} values were also evaluated using the experimental data of Kuebler and McKinley for the binary systems methane-n-butane, methane-n-pentane, methane-n-hexane for purposes of comparison.

The k_{ij} values obtained using the experimental data obtained in this work are listed in Table 5.5 and those for the experimental data of Kuebler and McKinley in Table 5.6. The average k_{ij} value for the methane-n-butane system was 0.0259 for our experimental data and 0.027 for the data of Kuebler and McKinley. For the system methane-n-pentane the

values were 0.0404 for our data and 0.0352 for the data of Kuebler and McKinley while for the methane-n-hexane system they were 0.0519 and 0.0814 respectively.

The critical properties, molecular weights, triple point properties for all the hydrocarbons were taken from the "Selected Values of Physical and Thermodynamic Properties of Hydrocarbons and Related Compounds" (20), with the exception of T_c and P_c for methane for which the values used were those reported by Prydz and Goodwin (15). The acentric factors used were those reported by Passut and Danner (21) since these were considered the most reliable to date.

TABLE 5.5

EXPERIMENTAL DATA (T, P, x_2) AND k_{ij} VALUES DETERMINED IN THIS INVESTIGATION

Temperature K	Pressure P psia	Mole Fraction of Solute x_2	k_{ij}
	n-Butane		
129.0	17.8	0.8115	0.0499
124.7	20.4	0.6938	0.0211
123.2	20.6	0.6811	0.0251
122.6	20.3	0.6460	0.0112
119.0	18.4	0.5315	0.0182
117.1	17.4	0.4334	0.0274
113.3	13.6	0.2830	0.0286
	n-Pentane		
131.25	49.2	0.4119	0.0397
130.2	48.0	0.3266	0.0420
129.4	47.3	0.2846	0.0410
128.1	43.8	0.1884	0.0404
127.8	42.8	0.1585	0.0405
125.9	38.4	0.0970	0.0388
123.4	33.4	0.0509	0.0403
	n-Hexane		
166.2	280.5	0.1795	0.0693
161.0	231.0	0.0640	0.0513
159.6	216.0	0.0409	0.0509

TABLE 5.5 (Cont'd)

Temperature K	Pressure P_{psia}	Mole Fraction of Solute x_2	k_{ij}
154.8	182.0	0.0292	0.0461
149.0	140.4	0.0120	0.0501
133.4	68.6	0.0044	0.044
	n-Octane		
179.7	484.6	0.0064	0.0317
173.9	398.7	0.0036	0.0375
166.0	297.0	0.0013	0.0503
156.3	198.0	0.0004	0.0613
	n-Nonane		
184.3	588.5	0.0018	0.1679
181.3	522.0	0.0013	0.0693
176.3	433.0	0.0010	0.0748
171.4	363.0	0.0005	0.0863

TABLE 5.6

EXPERIMENTAL DATA (T, P, x_2) OF KUEBLER AND MCKINLEY AND k_{ij} VALUES DETERMINED FROM THEIR DATA

Temperature K	Pressure P_{psia}	Mole Fraction of Solute x_2	k_{ij}
	n-Butane		
127.6	17.62	0.7760	0.0266
124.8	19.7	0.6868	0.0294
119.3	18.96	0.5101	0.0262
116.5	17.11	0.4137	0.0258
	n-Pentane		
139.8	28.77	0.826	0.0352
137.6	40.20	0.729	0.0274
133.2	49.60	0.508	0.0399
127.6	43.57	0.155	0.0377
122.0	31.44	0.0432	0.0359
116.5	21.12	0.0215	0.0352
	n-Hexane		
163.7	1393.76	0.1500	0.1141
162.6	1393.76	0.1110	0.080
162.0	1524.42	0.0783	0.1010
160.9	1524.42	0.05760	0.0895
158.1	1524.42	0.0348	0.0805
155.3	1524.42	0.0243	0.0787
149.7	1520.0	0.0135	0.0804

Temperature K	Pressure P_{psia}	Mole Fraction of Solute x_2	k_{ij}
144.2	1514.13	0.0082	0.0812
138.6	1514.13	0.0050	0.0839
133.0	1024.02	0.003	0.0531
127.4	1054.44	0.0018	0.0525

CHAPTER 6. DISCUSSION OF EXPERIMENTAL RESULTS, SUMMARY AND CONCLUSION

6.1 Discussion of Experimental Results

Kohn and Luks [4] in an attempt to shed some light on the solid-liquid-vapour (S-L-V) behaviour of systems encountered in the liquefaction of light hydrocarbons in a qualitative sense classified the phase behaviour of binary systems into four types. These four types of binary system phase behaviour are shown illustrated in Figure 6.1.

The solubility curves for Types A and B systems exhibit discontinuities while the solubility curves for Types C and D systems do not.

The discontinuity in the solubility curve of a Type A system is due to the presence of a solid-vapour gap in the solid-liquid-vapour locus of a Type A system. Methane-carbon dioxide, and methane-n-octane are typical Type A systems.

The discontinuity in the solubility curve of a Type B system (e.g. methane-n-heptane) is due to the presence of a quadruple Q-point, in the central portion of the solid-liquid-vapour locus for a Type B system. At this quadruple (S_2 - L_2 - L_1 - V) point, one loses the L_2 phase and gains an L_1 phase which is leaner in solute.

Types C and D systems have no discontinuities in the solid-liquid-vapour locus and consequently their solubility curves are continuous. The difference between Types C

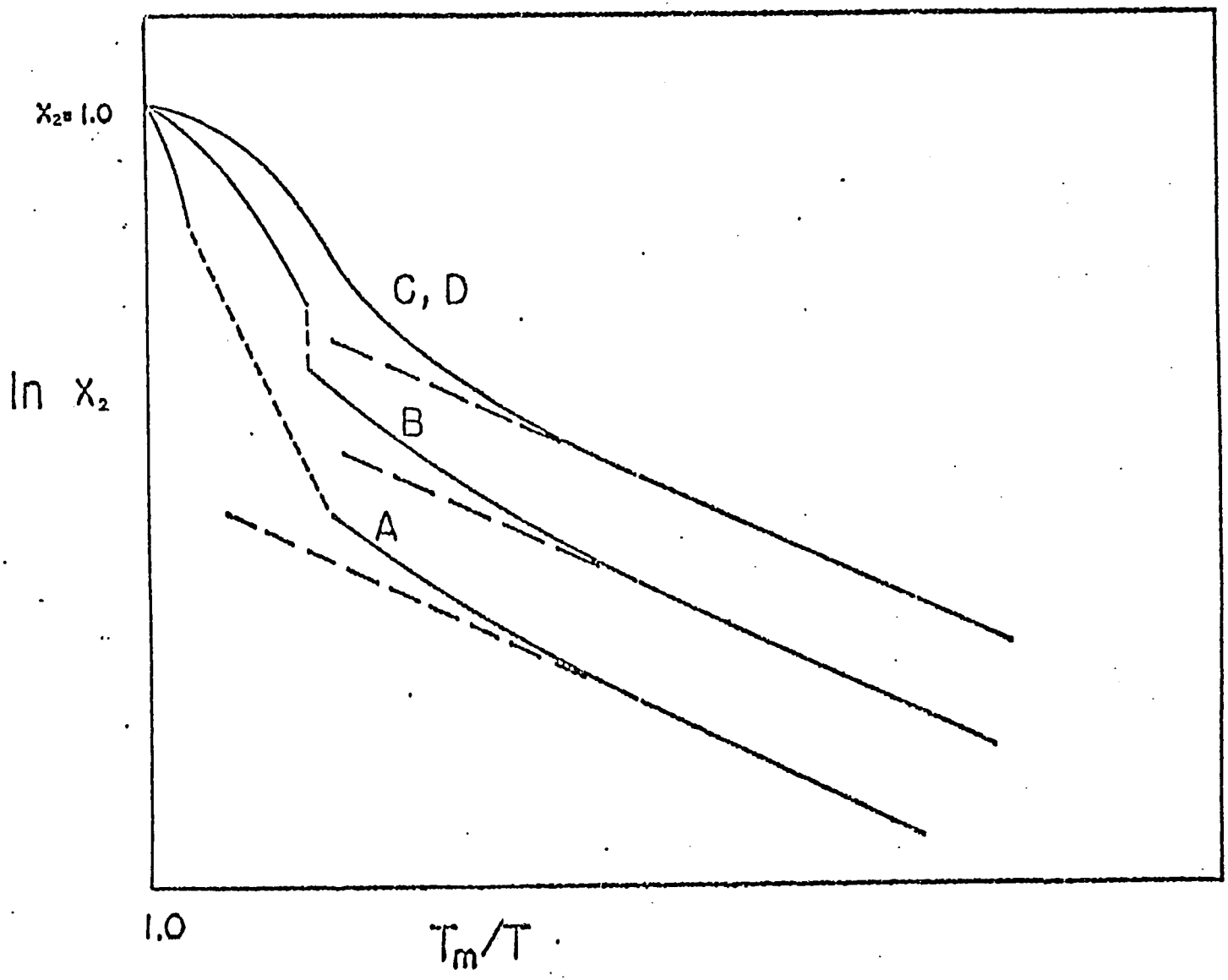

Figure 6.1 A Schematic Diagram of $\ell n\ x_2$ vs T_f/T for the Four Types of Binary System Behaviour Encountered in the Liquefaction of Light Hydrocarbons

and D systems is that a Type C system can exhibit liquid-liquid immiscibility whereas a Type D system does not. Methane-n-hexane is a typical Type C system while ethane-n-octane is a typical Type D system.

The experimental results obtained in this investigation are shown plotted together with the available literature, in Figures 4.3 to 4.7.

From the solubility plots (Figures 4.3 - 4.7) one sees that the solubility of solid hydrocarbons (n-butane and higher) decrease with increasing hydrocarbon number and decreasing temperature.

The solubility curves for the binary systems methane-n-butane, methane-n-pentane and methane-n-hexane exhibit no discontinuities and are therefore, using the classification of Kohn and Luks [4]. Type C or D systems. The solubility curves for the binary systems methane-n-octane and methane-n-nonane exhibit discontinuities and are therefore Type A systems. The existence of a solid-vapour gap in the solubility curve of the binary systems methane-n-octane, methane-n-nonane has been attributed [4] to the disparity in the solvent and solutes.

From the solubility plots (Figures 4.3 to 4.5), it is evident that our experimental data agree fairly well with the data of Kuebler and McKinley for the binary systems methane-n-butane, methane-n-pentane, and methane-n-hexane. It should be noted that the data of Kuebler and McKinley were obtained by the single pass continuous flow method which is

different from that used for this work.

Making precise measurements on the systems methane-n-octane, methane-n-nonane were difficult since

(i) solid deposition in the vapor recirculation line resulted in inadequate agitation of the cell contents.

(ii) the extremely low solute compositions made analysis of the samples on the gas chromatograph difficult and inaccurate. Owing to the low solute concentrations, gas chromatographic analysis had to be carried out at high sensitivity and this made the baseline unstable and consequently extremely difficult to distinguish between peaks due to electrical noise, voltage fluctuations and solute peaks.

A limited amount of ternary data were taken on the systems methane-ethane-n-hexane and methane-propane-n-hexane in an attempt to assess the solubility enhancement of solute hexane in liquid methane due to the presence of either ethane or propane. The data obtained are tabulated in Tables 4.8 and 4.9 and plotted in Figures 4.8 and 4.9.

From Figures 4.5, 4.8 and 4.9 one sees that at a temperature of 142.8 K the solubility of solid n-hexane in pure liquid methane is 0.007 mole fractions, while for the mixed solvents methane-ethane and methane-propane they are 0.0235 and 0.063 mole fractions respectively. Also at a temperature of 125. K, the respective solubilities were 0.0014,

0.0036 and 0.0107 mole fractions for pure liquid methane and the mixed solvents of methane-ethane and methane-propane.

Defining solubility enhancement (S.E.) at a given temperature as:

$$S.E. = \frac{\left(\begin{matrix}\text{Solubility in} \\ \text{Mixed Solvents}\end{matrix}\right) - \left(\begin{matrix}\text{Solubility in} \\ \text{Liquid Methane}\end{matrix}\right)}{\left(\text{Solubility in Liquid Methane}\right)} \qquad 6.1$$

the respective percentage solubility enhancements at 142.8 K are 253.7% for the mixed solvents of methane and ethane and 800% for the mixed solvents of methane and propane. At 125.0 K the respective solubility enhancements are 157.1% for the mixed solvents of methane and ethane and 664.3% for the mixed solvents of methane and propane.

6.2 Summary and Conclusion

The experimental results as presented in this work provided more data points for the following binary and ternary systems at the temperatures listed below.

System	Temperatures Investigated (K)
Methane-n-butane	129.0, 124.7, 123.2, 122.6, 119.0
Methane-n-pentane	131.25, 130.2, 129.4, 128.1, 127.8, 125.9, 123.4
Methane-n-hexane	166.2, 161.0, 159.6, 154.8, 149.0, 133.4
Methane-n-octane	179.7, 173.9, 166.0, 156.3
Methane-n-nonane	184.3, 181.3, 176.3, 171.4
Methane-ethane-n-hexane	154.8, 153.3, 150.7, 140.3, 134.9, 114.6

Methane-propane-n-hexane	153.0, 145.8, 135.6, 127.2, 120.4

Solid deposition at very low temperatures and the subsequent blockage of the return vapour line made adequate agitation of the cell contents extremely difficult. As a result of this, it was not possible to continue the data-taking to temperatures lower than those indicated above.

The difficulty of obtaining reliable results for the systems methane-n-octane, and methane-n-nonane was particularly great since these two solutes solidified and blocked the return vapour line long before the bath temperature was low enough to cause the liquefaction of methane. An attempt was made to solve this problem by raising the bath temperature after a sufficient quantity of liquid methane has been accumulated in the cell but this did not improve matters since when the temperature is raised, the liquid methane evaporates extremely rapidly and the cell pressure tended to exceed the maximum design limit of 600. psia which was dangerous. Also repeated cooling and heating of the cell resulted in leakages around the teflon gaskets.

From the percentage solubility enhancement at 142.8 and 125.0K respectively, it was found that the addition of either ethane or propane to liquid methane does enhance the solubility of n-hexane in liquid methane. The degree of enhancement is, however, higher with propane than with ethane.

In the correlation of the experimental results, the Redlich-Kwong Equation together with the proposed modified procedure previously proposed by Chang and Lu [11] was used. The values of the binary interaction constant k_{ij}, obtained using our experimental data and the experimental data of Kuebler and McKinley [5] show that k_{ij} is not a true constant since its values, for a given binary system, were different at different temperatures, pressures and compositions. A conclusion concerning the dependency of the binary interaction constant k_{ij} on the temperature, pressure and composition cannot, in our opinion, be based on the results of a single investigation. Further work need be done in order to make available sufficient data to enable a just conclusion to be drawn.

Finally, owing to the difficulty of making precise and reliable measurements at very low temperatures on the equipment used in this investigation, it is recommended that for any future endeavour aimed at extending the data range to very low temperatures, a new set-up, most probably based on the single pass continuous flow technique of Kuebler and McKinley[5] be constructed and used.

REFERENCES

1. Medici, M., "The Natural Gas Industry", p. 36, London-Newnes-Butterworths, (1974).

2. Preston, G.T., Funk, E.W. and Prausnitz, J.M., Ind. Eng. Chem. Process. Des. Dev. 9, 264, (1970).

3. Kurata, F., Gas Processors Assoc., Report RR-14 (1975).

4. Kohn, J.P. and Luks, K.D., Gas Processors Assoc. Research Report, RR-22 (1976).

5. Kuebler, G.P. and McKinley, C., Advances in Cryogenic Engineering 19, 320, (1974).

6. Denbigh, K., "The Principles of Chemical Equilibrium", p. 123, Cambridge University Press, London, U.K. (1961).

7. Prausnitz, J.M., "Molecular Thermodynamics of Fluid-Phase Equilibria", p. 386, 389, Prentice Hall, Inc. Englewood Cliffs, N.J., (1969).

8. Tiffin, D.L., Luks, K.D. and Kohn, J.P., Paper No. I. D.-6, (1977).

9. Hildebrand, J.H. and Scott, R.L., "Solubility of Non-Electrolytes", 3rd Edition, Dover Publications Inc., New York, (1964).

10. Redlich, O. and Kwong, J.N.S., Chem. Rev. 44, 233 (1949).

11. Chang, Shinder and Lu, B.C.-Y., Can. J. Chem. Eng. 48, 261 (1970).

12. Soave, G., Chem. Eng. Sci., 27, 1197, (1972).

13. De Mateo, A. and Kurata, F., Ind. Eng. Process. Des. Dev., Vol. 14, No. 2 (1975).

14. Haman, S.E.M. et. al., Ind. Eng. Chem. Process. Des. Dev., Vol. 16, No. 1, (1977).

15. Prydz, R. and Goodwin, R.D., J. Chem. Thermo. 4, 127, (1972).

16. Dietz, W.A., J. Gas. Chrom. 69, Feb., (1967).

17. Carruth, G.F. and Kobayashi, R., J. Chem. Eng. Data, 18, (2), 115, (1973).

18. Gunn, R.D. and Yamada, T., A.I.Ch.E. J. 17, (6), 1341, (1971).

19. Kato, M., Chung and Lu, B.C.-Y., Can. J. Chem. Eng., 54, No. 5, (1976).

20. Rossini, F.D., "Selected Values of Physical and Thermodynamic Properties of Hydrocarbons and Related Compounds", Carnegie Press, Pittsburg, Pa. (1953).

21. Passut, C.-A. and Danner, R.P., Ind. Eng. Chem. Process. Des. Dev. 12, 3 (1973).

22. Calingart, G. and Hitchcock, L.B., J. Am. Chem. Soc. 49, 750 (1927).

23. Hamam, S.E.M., M.A.Sc. Thesis, Univ. of Ottawa, (1972).

24. McNair, H.M. and Bonelli, E.J., Basic Gas Chromatography, p. 142, Gow Mack Instrument Company,

25. Yu, P., "Solubility Studies of Hydrocarbons in LNG for Alberta Research Council", Dept. of Chem. Eng., Univ. of Ottawa, (May 1975).

APPENDIX A

Calibration Curves

- Calibration curve for thermocouples
- Calibration curve for the binary system methane-n-butane.

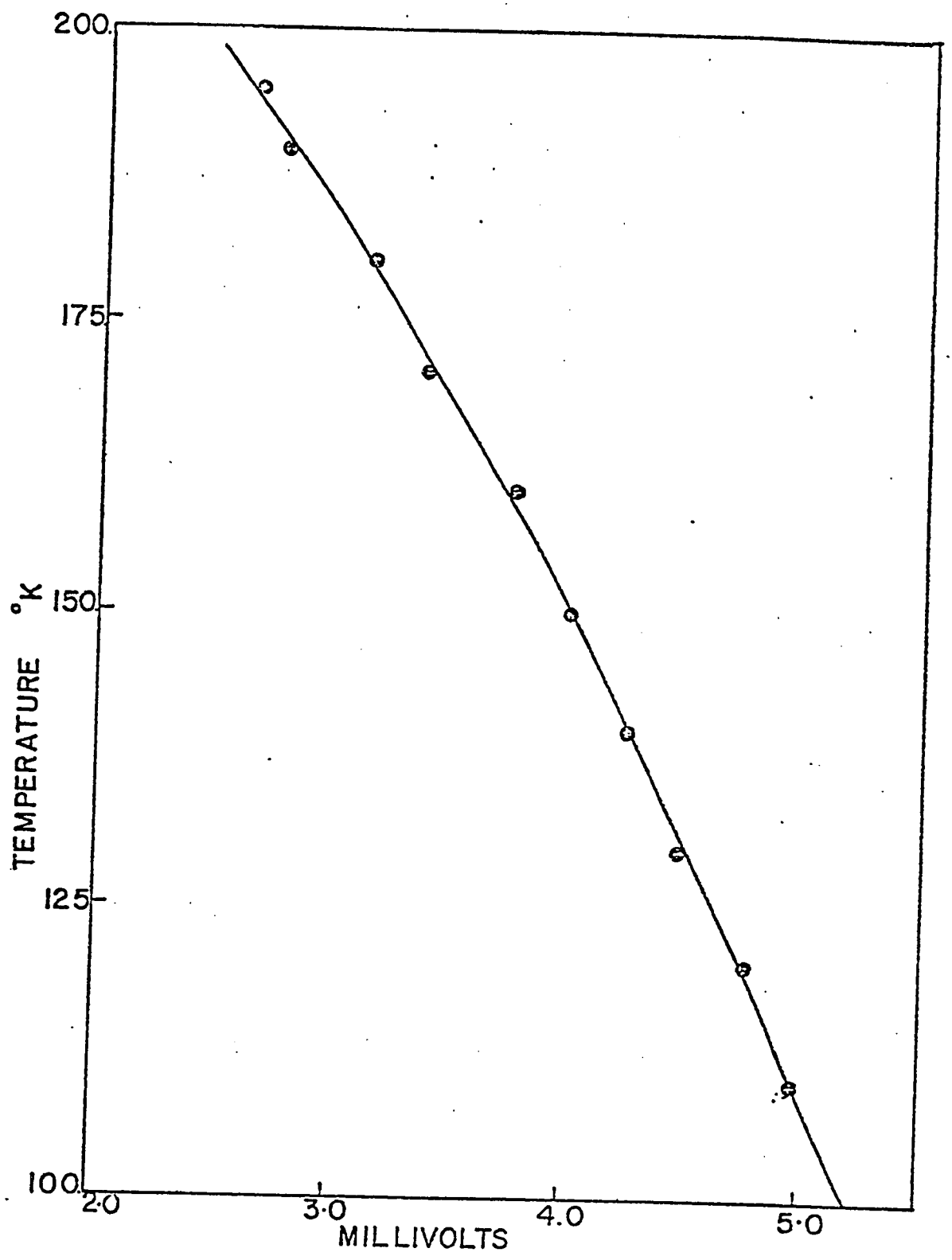

Calibration curve for the thermocouples

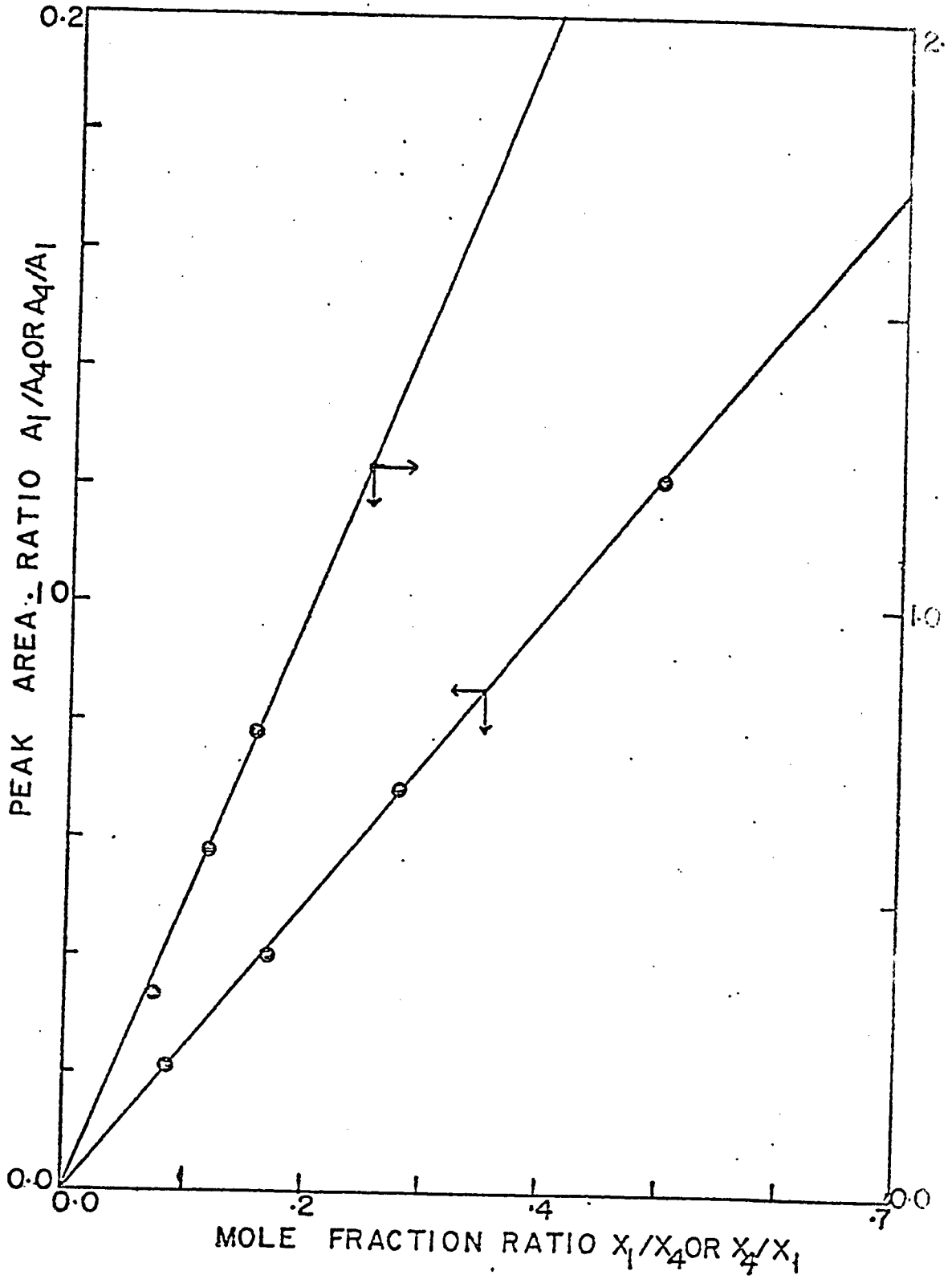

Calibration curves for the binary system

methane-n-butane

APPENDIX B

Computer Programs

- Evaluation of the parameters Ω_a, Ω_b of the Redlich-Kwong equation of state.
- Evaluation of the liquid phase activity for the solute γ_2, by means of the Redlich-Kwong equation of state.

```
LEVEL  21                    MAIN                    DATE = 77223          20/31/41
C
C
C     ***************************************************************
C     THIS  PROGRAM IS USED TO CALCULATE THE TEMPERATURE DEPENDENT
C     PARAMETERS OMEGA-A AND OMEGA-B OF THE REDLICH - KWONG EQUATION OF
C     STATE USING SATURATED LIQUID VOLUMES  PREDICIED USING THE GUNN -
C     YAMADA CORRELATION AND VAPOUR PRESSURES PREDICTED USING THE
C     CORRELATION OF CARRUTH AND KOBAYASHI.*****************************
C     ***************************************************************
C    EVALUATION OF WA AND WB BY ADJUSTING TC
C     ***************************************************************
      IMPLICIT REAL * 8 (A-H, O-Z)
       DIMENSION A0(20),A1(20), A2(20) ,B(20)
      DIMENSION TITLE(20)
      TOL = 0.5D-7
   23 READ (5, 100) (TITLE(I), I = 1, 15)
  100 FORMAT (20A4)
      WRITE (6, 200) (TITLE(I), I = 1, 15 )
  200 FORMAT (1H1, 'EVALUATION OF ADJUSTABLE PARAMETERS WA AND WB OF R-K
     1 EQN. FOR ',15A4//)
C          P IN MM OF MERCURY
C          T IN K
C          VL IN CM**3/MOLE
      READ(5, 111) TC,PC,VC,XMW
      READ(5, 101) DUMMY
  101 FORMAT (3D10.5,3I5)
      WRITE (6, 205) TC, PC
  205 FORMAT(1H0,'  TC=  ',D20.14,'   PC=',D20.14)
    1 READ(5,111) T,P,DUMMY,DUMMY,VL,KKK
  111 FORMAT(5F10.6,3I2)
      IF (T .LE. 0.D0) GO TO 23
      P = P/760
      N2 = 0
           R = 10.7315
      R = 1.3145
      R = 82.05606D0
      WRITE (6, 206) T, P , VL
  206 FORMAT(1H0,'
     1----------'//3X,'T=', D13.8, 3X, 'P=',D13.8, 3X, 'VL=',D13.8)
      WA0 = 1.0D0/(9.0D0*(2.0D0**(1.0D0/3.0D0)-1.0D0))
      WB0 =  (2.D0**(1.0D0/3.0D0)-1.0D0)/3.0D0
      ZL =  (VL/R)*(P/T)
      TR=T/TC
      PR=P/PC
      WRITE (6, 2003) ZL,TR,PR
 2003 FORMAT (3X,  'ZL=', D17.10,5X,'TR=',D15.8,5X,'PR=',D15.8/)
      IF ( ZL .GT. (1.0D0/3.0D0)) GO TO 26
  555 CONTINUE
      IF  (KKK.GE.2)      GO TO 8888
      GO TO 7777
 8888 WRITE   (6,388)
  388 FORMAT  (/10X,'CHECK THE INPUT DATA')
      GO TO 1
 7777 CONTINUE
      N = 1
      TC1 = TC
```

```
LEVEL  21                    MAIN                    DATE = 77223          20/31/41

   43 CONTINUE
  112 FORMAT(1H0, 3I5)
      N1 = 1
   10 F = (WA0/WB0)*(TC1/T )**1.5D0
        N2 = N2 + 1
C     DET IS DET/ZL
      DET = (1.D0-F)*(1.D0 - F) - 4.D0*(ZL+F)*(1.D0 - ZL)
      IF (DET)  41, 3, 4
    4 B1 = ((-(1.D0-F) + DSQRT(DET))/(2.D0*(F+ZL)))*ZL
      B2 = ((-(1.D0-F) - DSQRT(DET))/(2.D0*(F+ZL)))*ZL
C     FOR TEMPERATURE FAR FROM THE CRITICAL TEM. USE LARGE VALUE OF B
C     FOR TEM. NEAR THE CRITICAL  TEMP. USE SMALLER VALUE OF B
      IF  (KKK.EQ.0)       BX=B1
      IF  (KKK.EQ.1)       BX=B2
   33 AX = BX * F
      GO TO 28
    3 BX = -ZL*(1.D0-F)/(2.D0*(F+ZL))
      GO TO 33
   28 IF (BX) 27, 27, 24
   24 PC1 = P * (WB0/BX) * (TC1/T)
      IF ( T .GT. TC1 .OR. P .GT. PC1) GO TO 22
      C = AX - BX - BX*BX
      D = -AX*BX
        ZV1 = ZL
      C2 = 1.D0
      C1 = -(1.D0 - ZV1)
      C0 = C - (1.D0 - ZV1)*ZV1
      C3 = D + (C-(1.D0-ZV1)*ZV1)*ZV1
      IF (DABS(C3) .GT. TOL) GO TO 12
      DET = C1*C1 - 4.D0*C2*C0
      IF ( DET .LT. 0.D0) GO TO  41
      ZV2 = (-C1 + DSQRT(DET))/(2.D0*C2)
      ZV3 = (-C1 - DSQRT(DET))/(2.D0*C2)
      IF (ZV1 .LT. 0.D0 .OR. ZV2 .LT. 0.D0 .OR. ZV3 .LT. 0.D0) GO TO 13
      ZV = DMAX1 (ZV1, ZV2, ZV3)
      ZLC = DMIN1 (ZV1, ZV2, ZV3)
      IF ( DABS(ZL - ZLC) .GT. (TOL*10.D0)) GO TO 9
      IF ( BX/ZL - 1.D0) 29, 30, 30
   29 G = 1.0D0 - BX/ZL
      G1 = 1.D0 + BX/ZL
       PHILL= ZL - 1.D0 -DLOG(ZL) -DLOG(G) -(AX/BX)*DLOG(G1)
      G = 1.D0 - BX/ZV
      G1 = 1.D0 + BX/ZV
       PHIVL= ZV - 1.D0-DLOG(ZV) -DLOG(G) - (AX/BX)*DLOG(G1)
      PHIL = DEXP( PHILL)
      PHIV = DEXP( PHIVL)
       PLOVV = PHIL - PHIV
       PLOVVL = PHILL - PHIVL
      F1 =  PLOVVL
      WA = WA0*(PC/PC1)*(TC1/TC)**2.5D0
      WB = WB0*(TC1/TC)*(PC/PC1)
      TCK= TC1/TC
      PCK= PC1/PC
      IF ( N .EQ. 1) GO TO 21
      IF ( DABS(TC1-TC11) .GE. 1.D-7) GO TO 19
   25 CONTINUE
      KB=KKK+1
      WRITE(6,202)  KB, TC1, PC1,TCK,PCK, WA, WB, ZL, ZV,  PHIL,  PHIV,
```

```
LEVEL  21                    MAIN                    DATE = 77223          20/31/41

      1  PLOVV   ,N   ,N1  , N2
  202 FORMAT (3X ,'BX=',I1, 3X, 'TC1=', D13.8, 3X, 'PC1=', D13.8, 3X,
     1'TCK=', D13.8, 3X,'PCK=', D13.8, 3X, 'WA=', D13.8, 3X, 'WB=',D13.8
     2/ 3X, 'ZL=', D13.8, 3X, 'ZV=', D13.8, 3X, ' PHIL=',D17.8, 3X,
     3' PHIV=', D17.8, 3X, '  DPHI=', D17.10,3I3)
      WRITE(6, 1919) TR, WB
      WRITE(6, 1919) TR, WA
 1919 FORMAT(2D20.14)
      GO TO 1
   19 TC0 = TC1
      F0 = F1
      IF (DABS(F11 - F1) .LE. TOL*.1D-1) GO TO 42
      TC1 = TC1 - F1*((TC11-TC1)/(F11-F1))
      TC11 = TC0
      F11 = F0
      GO TO 20
   21 TC11 = TC1
      F11 = F1
      TC1 = TC1 * 1.0001D0
      GO TO 8
   22 CONTINUE
      TC1=1.001D0*TC1
       GO TO 44
   26 WRITE ( 6, 204) ZL
  204 FORMAT (1H , ' ERROR AND THE DATA DID NOT PROCESS DUE TO ZL GREATE
     1R THAN 0.33333333333')
      GO TO 1
   27 WRITE (3, 209)
  209 FORMAT (1H , 'ERROR DUE TO BX IS LESS THAN OR EQUAL TO ZERO')
      GO TO 1
   30 WRITE (6, 207)
  207 FORMAT ( 1H , 'ERROR DUE TO BX/ZL IS  EQUAL TO OR GREATER THAN 1')
      GO TO 1
   40 TC1 = TC1 * 1.0001D0
   20 IF ( N - 200) 8, 9, 9
    8 N = N + 1
      GO TO 43
   12 WRITE ( 6, 1003)
 1003 FORMAT (1H , 'REMAINDER IS DIFFERENT FROM ZERO')
      GO TO 1
   13 WRITE (6, 1004) ZV1, ZV2, ZV3
 1004 FORMAT (1H , 'AT LEAST ONE Z IS NEGATIVE', 3D17.10)
      GO TO 1
    9 CONTINUE
      KKK=KKK+1
      GO TO 555
   41 TC1 = 1.0001D0 * TC1
   44 IF ( N1 .GE. 200) GO TO 9
      N1 = N1 + 1
      GO TO 10
   42 WRITE (6, 1006) F11, F1
 1006 FORMAT (1H , 'DOUBLE ROOTS', 2D17.10)
        WRITE (6, 9119) F11, F1, TC11, TC1
 9119 FORMAT(1H ,4D20.8)
        GO TO 25
      END
```

```
C
C
C
C     *******************************************************************
C     THIS  PROGRAM  IS  USED  TO  CALCULATE  THE  BINARY  INTERACTION
C     CONSTANT KIJ SUCH THAT THE ACTIVITY COEFFICIENT CALCULATED FROM
C     PURE COMPONENT  PROPERTIES  IS  EQUAL  TO THE  ACTIVITY CALCULATED
C     FROM THE REDLICH- KWONG EQUATION OF STATE.************************
C     *******************************************************************
C
C
      DIMENSION  WA(2),WB(2),W(2),PC(2),VC(2),TC(2),AO(2),BO(2),AAO(2),
     1BBO(2),A(4),B(3),Z(3),VP(2),VL(2),X(2)
C
      COMMON /FIRST/ TC,PC,VC,W,T,P,R,NCOMP /SECOND/  Z,A,MTYPE
C
    1 READ (5,224)  PC(1),PC(2),VC(1),VC(2),TC(1),TC(2)
C
C
      READ (5,223) NCOMP   ,   R
  223 FORMAT (I5,F10.6)
C
    2 READ (5,224)  WA(1),WA(2),WB(1),WB(2),W(1),W(2),CORL
  224 FORMAT  (7F10.6)
C
      READ   (5,220)  VP(2),VL(2),X(2),X(1),ERROR
  220 FORMAT(F10.9,4F10.6)
C
C
C             READ  IN  SYSTEM  TEMPERATURER  PRESSURE
C
      READ(5,226)      T ,    PTOT ,   TM  ,   ENTF
  226 FORMAT  (4F10.6)
C
C            P  IS  IN  PSIA  CHANGE  TO  ATMOSPHERES
C
      P   =      PTOT   /   14.696
C             R  IS  IN  CUBIC  CENTIMETRES - ATM PER GM MOLE  DEG  KELVIN
      RR   =   R ** 2
      TT   =   T ** 2
      RT   =   R * T
      RRTT   =   RT  **2
C       CALCULATE A, B   R-K CONSTANTS FOR PURE COMPONENTS
C         WILL  NEED  A  DO  LOOP
C
      DO   33  I = 1, NCOMP
      AO(I)   =  WA(I)*RR*(TC(I)**2.5)/PC(I)
      BO(I)   =  WB(I)*R*TC(I)/PC(I)
C       CALCULATE   A**I  B  FOR  PURE  COMPONENTS
      AAO(I)   =   AO(I)/(RRTT* SQRT(T))
      BBO(I)   =   BO(I)/RT
   33 CONTINUE
      RCAL   =   1.987
      XGAM2   =   (1. -  TM/T)*ENTF/RCAL
      GAEX   =   EXP (XGAM2)
      GAM2   =   GAEX/X(2)
C
      WRITE (6,445)  GAM2
```

```
LEVEL  21                    MAIN                DATE = 77225          20/31/1
  445 FORMAT (1H/,'
     1------------'//10X,'ACTIVITY CALCULATED FROM  ENTF = ',D13.8)
C
C          CALCULATE  FUGACITY OF PURE SUBCOOLED  SOLUTE
C       VAPOUR PRESSURE OF SOLUTE IN  MM HG,  CHANGE  TO  ATMOS.
        VP2  =  VP(2)/760
C            EVALUATION  OF  ZL  FOR  PURE SUBCOOLED  SOLUTE
        ZL2  =  VP2*VL(2)/RT
        ZLL1  =  ZL2  -  1.
        ZLL2  =  ALOG (ZL2  -  BO(2)*VP2/RT  )
        ZLL3=ALOG(1.+BO(2)*VP2/(ZL2*RT))*(AO(2)/(BO(2)*R*T**1.5))
        PHIL  = ZLL1-ZLL2-ZLL3
        FUGG  =  EXP  (PHIL  )
        FUGL = EXP(PHIL)*VP2
C
        WRITE(6,177)  FUGL
  177 FORMAT(1H0,'
     1-------'//10X,'SAT,D FUGACITY OF X(2) = ',D13.8)
C
        FUGA  =  VL(2)  *  (  P  -  VP2  )  /  RT
        FUG1  =  EXP  (  FUGA  )
        FUG2  =  FUGL  *  FUG1
C
        WRITE  (6,888)       FUG2
  888 FORMAT(1H0,'
     1-------'//10X,'FUGACITY OF X(2)  AT PTOT & T SYS = ',D13.8)
C       CALCULATION OF TCIJ,V CIJ,PCIJ,AIK,ETC.
C            KIJ  =  CORL
        KKK  =  0
C
   53 I  =  1
        KKK  =  KKK  +  1
        IF  (  KKK .GE. 4000  )  GO  TO  55
        ALPHA  =  1.  -  CORL
        IF  (  ALPHA.LE.  0.  )  GO  TO  55
        TCIJ  =  (TC(I)*TC(I+1))**.5*(1.-CORL)
        WIJ  =  (W(I)  +  W(I+1))*.5
        ZCIJ  =  .291  -  .08 *  WIJ
        VCIJ  =  (VC(I)**(1./3.)  +  VC(I+1)**(1./3.))**3/8.
        PCIJ  =  ZCIJ  *  R  *TCIJ /VCIJ
        WAIJ  =  .5 * ( WA(I)  +  WA(I+1))
        AOIJ  =  WAIJ*RR*(TCIJ**2.5)/PCIJ
C
C        CALCULATE A**2,5, FOR  A  MIXTURE
        AMXIJ=
     1       AO(I)*(X(I)**2)+2*X(I)*X(I+1)*AOIJ+AO(I+1)*(X(I+1)**2)
        BMXIJ  =  BO(I)*X(I)  +  BO(I+1)*X(I+1)
C
C    CALCULATE  COEFFICIENTS  OF  CUBIC  EQUATION
        AA  =  AMXIJ/(RRTT  *  SQRT(T))
        BA  =  BMXIJ/RT
        A(1)  =  1.0
        A(2)  =  - 1.0
        A(3)  =  BA  *  P  *  (  AA  /  BA  -  1.  -  BA  *  P  )
        A(4)  =  -  (AA  /  BA  )  * (( BA  +  P  )  **  2  )
C        CALL  SUBROUTINE  CUBEQN
C
        CALL   CUBEQN
```

```
LEVEL  21                    MAIN                DATE = 77225          20/31/12
C
      ZL   =  AMIN1(Z(1),Z(2),Z(3))
      ZZL1   =  (ZL-1.)*BO(2)/BMXIJ
      ZZL2   =  ALOG(ZL-BMXIJ*P/RT)
      COEF1   =  AMXIJ/(BMXIJ*RT*T**.5)
      COEF2   =  (2.*X(2)*AO(2)+
     1                    2.*(1.- X(2))*AOIJ)/AMXIJ - BO(2)/BMXIJ
      TERM   =  ALOG ( 1.   +  BMXIJ * P / ZL / RT)
      TTA   =  COEF1 * COEF2 *TERM
      COEFL = ZZL1-ZZL2-COEF1*COEF2*ALOG(1.+BMXIJ*P/ZL/RT)
      ACT1   =  EXP  (  COEFL  )
      ACT2   =  ACT1  *  P  /  FUG2
C
C
      IF  (  ABS (ACT2-GAM2).LT.ERROR)  GO  TO  55
C
      IF  (ACT2  -  GAM2  ) 7,55,9
C
    7 CORL  =  CORL    +  .0001
C
      GO  TO  53
C
    9 CORL  =  CORL  -  .0001
C
      GO  TO  53
C
C
   55 WRITE (6,899)  ACT2,CORL,PTOT,T,X(2),ERROR,P,KKK
  899 FORMAT(1H0,'
     1-------'//10X,'ACTIVITY FROM R-K EQN.=',D13.6,5X,'KIJ=',D19.6,//10
     2X,' PTOT = ',D13.6,10X,'TEMP=   ',D13.6,3X,'X(2) = ',D13.6,3X,'ERR
     3OR = ',D13.6/3X,'P=',D13.6,3X,'KKK = ',I8)
C
C
      GO  TO  2
C
      END
```

```
LEVEL  21                    MAIN                DATE = 77223          20/31/12
C     ***************************************************************
      SUBROUTINE CUBEQN
C   SOLVES CUBIC EQUATION OF REDLICH-KWONG EQUATION
C     FOR COMPRESSIBILITY FACTORS
C     ***************************************************************
      DIMENSION A(4),Z(3) ,B(3)
      COMMON /SECOND/ Z,A,MTYPE
    1 CONTINUE
      B(1)=A(2)/A(1)
      B1OV3=B(1)/3.0
      B(2)=A(3)/A(1)
      B(3)=A(4)/A(1)
      ALF=B(2)-B(1)*B1OV3
      BET=2.0*B1OV3**3  -B(2)*B1OV3+B(3)
      BETOV2=BET/2.0
      ALFOV3=ALF/3.0
      CUAOV3=ALFOV3**3
      SQBOV2=BETOV2**2
      DEL=SQBOV2+CUAOV3
      IF(DEL)40,20,30
   20 MTYPE=0.0
      GAM=SQRT(-ALFOV3)
      IF(BET)22,22,21
   21 Z(1)=-2.0*GAM-B1OV3
      Z(2)=GAM-B1OV3
      Z(3)=Z(2)
      GO TO 50
   22 Z(1)=2.0*GAM-B1OV3
      Z(2)=-GAM-B1OV3
      Z(3)=Z(2)
      GO TO 50
   30 MTYPE=1
      EPS=SQRT(DEL)
      TAU=-BETOV2
      RCU=TAU+EPS
      SCU=TAU-EPS
      SIR=1.0
      SIS=1.0
       IF(RCU)31,32,32
   31 SIR=-1.0
   32 IF(SCU)33,34,34
   33 SIS=-1.0
   34 R=SIR*(SIR*RCU)**0.33333333
      S=SIS*(SIS*SCU)**0.33333333
      Z(1)=R+S-B1OV3
      Z(2)=-(R+S)/2.0-B1OV3
      Z(3)=0.86602540*(R-S)
      GO TO 50
   40 MTYPE=-1
      QUOT=SQBOV2/CUAOV3
      ROOT=SQRT(-QUOT)
      IF(BET)42,41,41
   41 PEI=(1.5707963+ATAN(ROOT/SQRT(1.0-ROOT**2)))/3.0
      GO TO 43
   42 PEI=ATAN(SQRT(1.0-ROOT**2)/ROOT)/3.0
   43 FACT=2.0*SQRT(-ALFOV3)
      Z(1)=FACT*COS(PEI)-B1OV3
      PEI2=PEI+2.0943951
```

```
LEVEL  21                    CUBEQN                  DATE = 77223          20/31/12
      Z(2)=FACT* COS(PEI2)                -B10V3
      PEI4=PEI+4.1887902
        Z(3)=FACT* COS(PEI4)                -B10V3
   50 RETURN
      END
```

APPENDIX C

SAMPLE CALCULATION

C.1 Conversion of Peak Areas into Mole Fraction Using Relative Sensitivity Factors

Areas of compounds are not directly proportional to percent composition i.e., different compounds have different detector responses; therefore, it is necessary to determine correction factors. Once determined, these correction factors can be used to calculate the percent composition. Since detectors operate on different principles, different factors must be calculated for different detectors.

An excellent reference for response factors for both flame ionization and thermal conductivity detectors is the article by Dietz [16].

The gas chromatograph used to analyze the vaporized liquid samples taken in this investigation is equipped with a flame ionization detector (FID). The response of a FID is independent of temperature, carrier gas, and flow rate. This makes it well suited, possibly the best detector for quantitative analysis. For weight percent calculations the response factors reported by Dietz [24] can be used. The calculational procedure is as follows:

Step No. 1

Compound	Area (cm^2)	Relative Sensitivity
Methane	126,739	0.97
Pentane	215,636	1.04

Divide the peak areas by relative sensitivity.

Step No. 2

Methane $(126{,}739/_{0.97})$ = 130,658.7629

Pentane $(215{,}636/_{1.04})$ = 207,342.3077

Total = 338,001.0706

Now normalize and the answer is weight %

$$\% A = \frac{\text{Area of } A/_{Fa}}{\Sigma \text{ Area}/_{\text{Factors}}} \times 100$$

Weight % Methane = 38.6563

Weight % Pentane = 61.3437

Step No. 3

Conversion of weight % to mole fractions.

Basis: 100 lbs

lbs Methane = 38.6563

lbs Pentane = 61.3437

Moles Methane = 2.4099

Moles Pentane = 0.8502

Total = 3.2602

$$\text{Mole Fraction A} = \frac{\text{Moles A}}{\text{Total Moles}}$$

Mole Fraction Methane = 0.7392

Mole Fraction Pentane = 0.2608

APPENDIX D

RESULTS OF A TYPICAL ANALYSIS

Temperature = 113.3 K

Pressure = 13.6 psia

Number of samples = 5

SAMPLE NO. 1

Injection Number M	Peak Area Methane A_1 A x $10^{N\downarrow}$		Peak Area n-Butane A_4 A x $10^{N\downarrow}$		Peak Area Ratio A_{4/A_1}
1	9813	1	1820	2	1.8547
2	1006	2	1876	2	1.8648
3	1170	2	2300	2	1.9658
4	9848	1	1870	2	1.8989
5	1068	2	1910	2	1.7884
6	1131	2	2165	2	1.9142
7	1235	2	2315	2	1.8745
8	1034	2	1909	2	1.8462
9	1021	2	1930	2	1.8903
10	1023	2	1927	2	1.8837
11	1015	2	1815	2	1.7882
12	1122	2	2116	2	1.8859
13	1017	2	1917	2	1.8850
14	1046	2	1949	2	1.8633
15	9768	1	1870	2	1.9144

Average Peak Area Ratior for Sample No. 1 $\left(A_{4/A_1}\right)_{AVG}$ = 1.8746.

From calibration curve (p. 92) the corresponding mole fraction ratio X_{4/X_1} is 0.3802.

Now $\frac{X_4}{X_1} = 0.3802$ - D-1

Also for the binary system methane (1)-n-butane(2), the sum of the mole fractions ($X_1 + X_4$) equals unity i.e.

$$X_1 + X_4 \text{ - D-2}$$

From the equations D-1 and D-2, we obtain $X_1 = 0.7245$

and $X_4 = 0.2755$

∴ Mole fraction butane = 0.2755

Mole fraction methane = 0.7245

SAMPLE NO. 2

Injection Number M	Peak Area Methane A_1 A x $10^{N\downarrow}$		Peak Area n-Butane A_4 A x $10^{N\downarrow}$		Peak Area Ratio A_4/A_1
1	1030	2	2034	2	1.9748
2	1030	2	2044	2	1.9845
3	1062	2	2103	2	1.9802
4	1051	2	2004	2	1.9068
5	1109	2	2222	2	2.0036
6	1020	2	2017	2	1.9774
7	1075	2	2110	2	1.9628
8	1043	2	2001	2	1.9185
9	1068	2	2113	2	1.9785
10	1007	2	2009	2	1.9950
11	1002	2	2018	2	2.0140
12	9938	1	2044	2	2.0567
13	9756	1	1919	2	1.9669
14	9935	1	1912	2	1.9245
15	9971	1	2002	2	2.0078

Average Peak Area Ratio for Sample No. 2 $\left(\frac{A_4}{A_1}\right)_{AVG}$ = 1.9768.

Mole Fraction Ratio $\left(\frac{X_4}{X_1}\right)$ = 0.4009

$\therefore$ X_4 = 0.2862

X_1 = 0.7138

SAMPLE NO. 3

Injection Number M	Peak Area Methane A_1 A x $10^{N\downarrow}$		Peak Area n-Butane A_4 A x $10^{N\downarrow}$		Peak Area Ratio $\frac{A_4}{A_1}$
1	1030	2	2034	2	1.9748
2	1121	2	2144	2	1.9126
3	1045	2	2105	2	2.0143
4	1002	2	2217	2	2.2126
5	1054	2	2123	2	2.0142
6	1016	2	2075	2	2.0423
7	9930	1	2040	2	2.0544
8	1006	2	2126	2	2.1133
9	1013	2	2074	2	2.0474
10	9904	1	2066	2	2.0860
11	1014	2	2074	2	2.0454
12	1026	2	2102	2	2.0487
13	9919	1	2044	2	2.0607
14	1078	2	2133	2	1.9787
15	1000	2	1917	2	1.9170
16	1004	2	1937	2	1.9293

Average Peak Area Ratio for Sample No. 3 $\left(\frac{A_4}{A_1}\right)_{AVG}$ = 2.0282.

Mole Fraction Ratio $\left(X_{4/X_1}\right)$ = 0.4114.

$\therefore$ Mole Fraction n-Butane X_4 = 0.2915.

Mole Fraction Methane X_1 = 0.7085.

SAMPLE NO. 4

Injection Number M	Peak Area Methane A_1 A x $10^{N\downarrow}$		Peak Area n-Butane A_4 A x $10^{N\downarrow}$		Peak Area Ratio $\frac{A_4}{A_1}$
1	9567	1	1973	2	2.0623
2	1206	2	2604	2	2.1592
3	1028	2	1926	2	1.8735
4	1067	2	1976	2	1.8519
5	9923	1	1879	2	1.8936
6	9449	1	1933	2	2.0457
7	9207	1	1817	2	1.9735
8	1022	2	1944	2	1.9021
9	1005	2	1816	2	1.8070
10	9379	1	1823	2	1.9437

Average Peak Area Ratio for Sample No. 4 $\left(A_4/A_1\right)_{AVG}$ = 1.9513.

Mole Fraction Ratio X_4/X_1 = 0.3958.

Mole Fraction n-Butane (X_4) = 0.2836.

Mole Fraction Methane (X_1) = 0.7164.

SAMPLE NO. 5

Injection Number M	Peak Area Methane A_1 A x 10^N		Peak Area n-Butane A_4 A x 10^N		Peak Area Ratio A_4/A_1
1	1039	2	1956	2	1.8826
2	1048	2	1954	2	1.8645
3	1033	2	1956	2	1.8935
4	1076	2	2026	2	1.8829
5	1028	2	1955	2	1.9017
6	1056	2	2008	2	1.9015
7	1017	2	1954	2	1.9213
8	1042	2	1901	2	1.8244
9	9778	1	1869	2	1.9114
10	1016	2	2053	2	2.0207
11	1012	2	1946	2	1.9229
12	1049	2	1970	2	1.8779
13	1019	2	1953	2	1.9166

Average Peak Area Ratio for Sample No. 5 $\left(A_4/A_1\right)_{AVG} = 1.9017.$

Mole Fraction Ratio $\left(\frac{X_4}{X_1}\right) = 0.3857.$

Mole Fraction n-Butane $X_4 = 0.2784.$

Mole Fraction Methane $X_1 = 0.7216.$

The average mole fraction for these five samples for n-Butane is 0.2830. Hence the solubility of n-butane in liquid methane at T = 113.3 K, P = 13.6 psia. is 0.2830 of a mole fraction.

The procedure outlined above was used in the determination of the mole fraction for the other experimental conditions.

APPENDIX E

TABLE E-1

EXPERIMENTAL DATA (T, P, X_2), ACTIVITY COEFFICIENT (γ_2) AND K_{ij} VALUES DETERMINED IN THIS INVESTIGATION

Temp. K	Pressure P psia	Mole Fraction Solute X_2	Activity Coefficient γ_2 Calculated from Equ. 3.30	Activity Coefficient γ_2 R-K Calculated Using Redlich-Kwong Equation of State	K_{ij}
			n-BUTANE		
129.0	17.8	0.8115	1.0219	1.0201	0.0499
124.7	20.4	0.6938	1.0289	1.0299	0.0211
123.2	20.6	0.6811	1.0521	1.0531	0.0251
122.6	20.3	0.6460	1.0232	1.0241	0.0112
119.0	18.4	0.5315	1.0830	1.0837	0.0182
117.1	17.4	0.4334	1.2305	1.2302	0.0274
113.3	13.6	0.2830	1.6049	1.6056	0.0286
			n-PENTANE		
131.25	49.2	0.4119	1.2597	1.2599	0.0397
130.2	48.0	0.3266	1.4933	1.4936	0.0420
129.4	47.3	0.2846	1.6329	1.6326	0.0410
128.1	43.8	0.1884	2.2795	2.2794	0.0404
127.8	42.8	0.1585	2.6592	2:6537	0.0405
125.9	38.4	0.0970	3.8557	3.8603	0.0388
123.4	33.4	0.0509	6.2504	6.2402	0.0403

TABLE E-1 (Cont'd)

Temp. K	Pressure P psia	Mole Fraction Solute X_2	Activity Coefficient γ_2 Calculated from Equ. 3.30	Activity Coefficient γ_2 R-K Calculated Using Redlich-Kwong Equation of State	K_{ij}
			n-HEXANE		
166.2	280.5	0.1795	3.0092	3.0119	0.0693
161.0	231.0	0.0640	6.2218	6.2054	0.0513
159.6	216.0	0.0409	8.9337	8.9317	0.0509
154.8	182.0	0.0292	9.2278	9.2404	0.0461
149.0	140.4	0.0120	15.1122	15.0952	0.0501
133.4	68.6	0.0044	12.2285	12.2478	0.044
			n-OCTANE		
179.7	484.6	0.0064	14.9507	14.9372	0.0317
173.9	398.7	0.0036	16.5535	16.5132	0.0375
166.0	297.0	0.0013	23.4506	23.5442	0.0503
156.3	198.0	0.0004	30.8397	30.9069	0.0613
			n-NONANE		
184.3	588.5	0.0018	106.5246	106.5256	0.1679
181.3	522.0	0.0013	131.303	131.120	0.0693
176.3	433.0	0.0010	124.65	124.921	0.0748
171.4	363.0	0.0005	174.931	174.178	0.0863

TABLE E-2

EXPERIMENTAL DATA (T, P, X_2) OF KUEBLER AND McKINLEY AND ACTIVITY COEFFICIENTS (γ_2) AND K_{ij} VALUES DETERMINED FROM THEIR DATA

Temp. K	Pressure P psia	Mole Fraction Solute X_2	Activity Coefficient γ_2 Calculated from Equ. 3.30	Activity Coefficient γ_2 R-K Calculated Using Redlich-Kwong Equation of State	K_{ij}
			n-BUTANE		
127.6	17.62	0.7760	1.0181	1.01715	0.0266
124.8	19.7	0.6868	1.0432	1.0441	0.0294
119.3	18.96	0.5101	1.1419	1.1425	0.0262
116.5	17.11	0.4137	1.2577	1.2580	0.0258
			n-PENTANE		
139.8	28.77	0.826	1.0054	1.0062	0.0352
137.6	40.20	0.729	1.015	1.016	0.0274
133.2	49.60	0.509	1.1431	1.1437	0.0399
127.6	43.57	0.155	2.686	2.688	0.0377
122.0	31.44	0.0432	6.7032	6.6839	0.0359
116.5	21.12	0.0215	9.1131	9.0949	0.0352
			n-HEXANE		
163.7	1393.76	0.1500	3.1188	3.1195	0.1141
162.6	1393.76	0.1110	3.9503	3.9513	0.0800
162.0	1524.42	0.0783	5.4037	5.4045	0.1010
160.9	1524.42	0.0576	6.8757	6.8764	0.0895
158.1	1524.42	0.0348	9.5775	9.5785	0.0805
155.3	1524.42	0.0243	11.4716	11.4724	0.0787
149.7	1520.0	0.0135	14.1572	14.1576	0.0804
144.2	1514.13	0.0082	15.7122	15.7118	0.0812
138.6	1514.13	0.0050	16.5967	16.5976	0.0839
133.0	1024.02	0.003	17.3471	17.4284	0.531
127.4	1054.44	0.0018	17.1867	17.1122	0.525